European Journal of Medicinal Chemistry 115 (2016) 326–341

Contents lists available at ScienceDirect

European Journal of Medicinal Chemistry

journal homepage: http://www.elsevier.com/locate/ejmech

Research paper

Novel $S1P_1$ receptor agonists – Part 5: From amino-to alkoxy-pyridines

Martin H. Bolli*, Cyrille Lescop, Magdalena Birker, Ruben de Kanter, Patrick Hess, Christopher Kohl, Oliver Nayler, Markus Rey, Patrick Sieber, Jörg Velker, Thomas Weller, Beat Steiner

Actelion Pharmaceuticals Ltd., Gewerbestrasse 16, CH-4123 Allschwil, Switzerland

ARTICLE INFO

Article history:
Received 21 August 2015
Received in revised form
7 March 2016
Accepted 9 March 2016
Available online 12 March 2016

Keywords:
$S1P_1$ receptor agonist
Pyridine
Lymphocyte count
Immunomodulation
In vitro phototoxicity
Light extinction

ABSTRACT

In a previous communication we reported on the discovery of aminopyridine **1** as a potent, selective and orally active $S1P_1$ receptor agonist. More detailed studies revealed that this compound is phototoxic *in vitro*. As a result of efforts aiming at eliminating this undesired property, a series of alkoxy substituted pyridine derivatives was discovered. The photo irritancy factor (PIF) of these alkoxy pyridines was significantly lower than the one of aminopyridine **1** and most compounds were not phototoxic. Focused SAR studies showed, that 2-, 3-, and 4-pyridine derivatives delivered highly potent $S1P_1$ receptor agonists. While the 2-pyridines were clearly more selective against $S1PR_3$, the corresponding 3- or 4-pyridine analogues showed significantly longer oral half-lives and as a consequence longer pharmacological duration of action after oral administration. One of the best compounds, cyclopentoxy-pyridine **45b** lacked phototoxicity, showed EC_{50} values of 0.7 and 140 nM on $S1PR_1$ and $S1PR_3$, respectively, and maximally reduced the blood lymphocyte count for at least 24 h after oral administration of 10 mg/kg to Wistar rats.

1. Introduction

Sphingosine-1-phosphate (S1P) is a lysophospholipid affecting fundamental cellular processes including cell survival, differentiation, proliferation or migration [1–4]. In the cell, S1P is produced from the lipid component ceramide. Ceramidase cleaves ceramides to give sphingosine which is phosphorylated by one of two sphingosine kinases to form S1P. Lipid phosphate phosphatase and other phosphatases can hydrolyze S1P back to sphingosine and thus inactivate it. S1P may also be cleaved irreversibly by S1P lyase to hexadecanal and aminoethanol phosphate making it unavailable for reactivation by sphingosine kinases. S1P is transported out of the cell to convey its biological activity in an autocrine or paracrine fashion. Extracellular S1P exerts its activity by signalling through five G-protein coupled receptors ($S1PR_{1-5}$). S1P concentrations greatly vary depending on the body compartment. For instance, while S1P is stored in erythrocytes, endothelial cells, and plasma lipoproteins, and its concentrations are high in plasma (up to nearly 1 μM) and in lymph but low in tissue [1,5,6]. As maintenance of this concentration gradient is fundamental to the biological function of S1P, its synthesis, degradation, transport and storage are tightly regulated [7–11].

While the physiological effects of S1P–S1P receptor signalling have been studied in many organs and tissues [1] including the nervous system [12,13], the lung [14,15], the cardiovascular system [7,16–18] bone tissue [19], and haematopoietic and immune cells [20–23], the observation that lymphocytes exposed to a synthetic $S1P_1$ receptor agonist are sequestered to lymphoid organs, removed from circulation and are thus unable to aberrantly cause tissue damage [24–26] is of particular interest. This novel mechanism of immunomodulation [26–28] holds great promise in the fields of transplantation and autoimmune diseases [29]. Today, fingolimod (Gilenya®), a prodrug of a non-selective S1P receptor agonist, is a successfully used approved therapy to treat relapsing multiple sclerosis [30–34]. In addition, clinical use of $S1P_1$ receptor agonists in other autoimmune diseases is being evaluated [35–40].

Detailed mechanistic studies suggest that synthetic $S1P_1$ receptor agonists in fact act as functional antagonists [41–45]. Rapid and sustained internalization of the $S1P_1$ receptor upon stimulation abolishes the lymphocyte's ability to sense and migrate along the

* Corresponding author.
E-mail address: martin.bolli@actelion.com (M.H. Bolli).

http://dx.doi.org/10.1016/j.ejmech.2016.03.020
0223-5234/

S1P gradient it needs to follow in order to exit the lymph node. In view of this mode of action, it was postulated that also $S1P_1$ receptor antagonists are able to sequester lymphocytes to lymph nodes. However, this hypothesis was proven only recently [46–50]. On the other hand, it was recently demonstrated that disturbing the S1P gradient by blocking the activity of S1P lyase with a synthetic inhibitor can lead to lymphocyte sequestration too [51]. How $S1PR_1$ antagonists and S1P lyase inhibitors compare to $S1PR_1$ agonists with respect to clinical efficacy and safety is of great interest and results of on-going and future studies are eagerly awaited [5,52,53].

Our interest to identify novel S1P receptor agonists is based on the following observations: Experiments with $S1PR_1$ receptor knock-out mice [54,55] and $S1PR_1$ selective agonists [44,56,57], revealed that targeting $S1PR_1$ is sufficient to cause lymphocyte sequestration to lymphoid organs. Originally, $S1P_1$ receptor agonism-triggered lymphocyte sequestration [43,54,58] was proposed as the driving mechanism for the efficacy of S1P receptor agonists in experimental autoimmune encephalomyelitis (EAE) models in rodents [59–61]. More recent studies suggested that $S1P_1$ receptor modulation on neurons and astrocytes also contributes to the efficacy in these multiple sclerosis models [31,62–64]. On the other hand, activation of $S1P_5$ receptors on astrocytes may enhance remyelination [65]. In contrast to these beneficial effects of $S1P_1$ and $S1P_5$ receptor agonism, $S1P_3$ receptor activation is associated with heart rate reduction [58,66–68], vaso- and bronchoconstriction [66,69], blood pressure increase [70], and fibrosis [71] in rodents and is thus deemed undesired. As a consequence, the majority of the corresponding drug discovery programs [72–74], including our own, focused on identifying potent $S1P_1$ receptor agonists with high selectivity against $S1PR_3$ and variable degrees of activity on $S1PR_5$.

In a previous communication [75] we reported on the discovery of amino-pyridine **1** as a potent and selective $S1P_1$ receptor agonist with high efficacy in reducing blood lymphocyte counts in the rat. In more detailed studies involving a standardized Neutral Red Uptake Phototoxicity Test using Balb/c 3T3 mouse fibroblasts (3T3 NRU) [76,77], the photo irritancy factor (PIF) of aminopyridine **1** was found to be >200, clearly flagging this compound as *in vitro* phototoxic [78]. Testing of additional examples of our $S1PR_1$ agonists incorporating a pyridine head suggested that the phototoxicity is an inherent property of the aminopyridine series. For instance, while aminopyridines such as **1**, **2** and **3** were clearly phototoxic *in vitro*, dialkyl pyridine analogues such as compounds **4**, **5** [75], and **6** [79] were devoid of this undesired property (Fig. 1). Our discovery efforts therefore aimed at identifying novel $S1P_1$ receptor agonists that combined the high affinity and selectivity for $S1PR_1$ and the favourable *in vivo* efficacy of the aminopyridine series [75] with the lack of the phototoxicity liability observed for the dialkyl pyridine derivatives.

Health authority guidelines e.g. Refs. [80,81], recommend *in vitro* photosafety assessment for compounds with a molar extinction (ε) of >1000 L mol^{-1} cm^{-1} at wavelengths >290 nm. As the phototoxic aminopyridines **1**, **2**, and **3** as well as the non-phototoxic analogues **4**, **5**, and **6** fulfilled this criterion, measuring the molar extinction at >290 nm offered no guidance for our medicinal chemistry program. In a recent computational approach described by Haranosono et al. [82], the energy difference between the HOMO and LUMO (HOMO–LUMO gap, HLG) and the maximum-conjugated π electron number (PENMC) were calculated to predict the compound's phototoxicity potential. However, applying this *in silico* method to our pyridine derivatives, we were not able to explain the clear difference between the measured PIF values of the aminopyridine and the dialkyl pyridine series as both series were clearly predicted to be phototoxic. Hence, while staying pragmatic, we wondered whether replacing one of the two alkyl groups in the dialkyl pyridine series by an alkoxy group would again produce compounds with no phototoxicity liability. A first alkoxy pyridine, the 2-methoxy-isonicotinic acid derivative **7a**, showed a PIF value of 0.9 in the 3T3 NRU phototoxicity test, demonstrating that it is not phototoxic *in vitro*. Interestingly, during the synthesis of **7a** we also noted that aminopyridines such as **1**, **2**, and **3** were strongly fluorescent under UV light (254 nm and 366 nm) when spotted on thin layer chromatography plates while the dialkyl pyridine **4**, **5**, and **6** as well as the methoxy pyridine **7a** were devoid of this property. On this basis, we set out to explore the alkoxy pyridines in more detail.

2. Results and discussion

2.1. Chemistry

The target compounds **7a**–**k**, **24a**–**g**, **35a**,**b**, and **45a**–**d** were prepared in analogy to a previously reported pathway [75]. Thus, as summarized in Scheme 1 the isonicotinic acids **12a**–**k**, the picolinic acids **23a**–**g** and **34a**,**b**, and the nicotinic acids **44a**–**d** were coupled with *N*-hydroxy-benzamidine **8** or **9** and the resulting amidine ester intermediates were cyclized to the desired oxadiazoles. In case hydroxyamidine **8** was used, the desired polar side chain (R_1) was established in steps that followed the cyclization step (for details see Supporting information).

Schemes 2–5 summarize the synthetic pathways that were followed to obtain the various pyridine carboxylic acid derivatives required for this study. In general, yields have not been optimized. For details see Supporting information.

The synthesis of the 2,6-disubstituted isonicotinic acids **12a**–**k** required to produce target compounds **7a**–**k** is illustrated in Scheme 2. Reacting methyl or ethyl 6-chloro-2-methoxyisonicotinate **10** with an alkylmagnesium halide under Fürstner conditions [83,84] furnished the corresponding 6-alkyl-2-methoxy-isonicotinates **11a**, **11b**, and **11d**. Alternatively, 6-alkyl-2-methoxy-isonicotinic acid esters **11c** and **11e** were prepared by reacting methyl or ethyl 6-chloro-2-methoxyisonicotinate with the appropriate cycloalkylzinc bromide under Negishi conditions [85–87]. Methyl 2-methoxy-6-phenylisonicotinate **11f** was obtained by $Pd(PPh_3)_4$ catalyzed Suzuki coupling [87,88] of methyl 6-chloro-2-methoxyisonicotinate with phenylboronic acid. The desired isonicotinic acids **12a**–**f** were then obtained by cleavage of the corresponding esters using concentrated aqueous HCl or aqueous NaOH or LiOH.

On the other hand, reacting 2-chloro-6-methylisonicotinic acid **13** with isopropanol under basic conditions gave access to 2-isopropoxy-6-methylisonicotinic acid **12g**. As illustrated with isonicotinic acids **12h**–**12k**, 2-alkoxy-6-alkylisonicotinic acids could also be prepared by an alternative pathway giving access to isonicotinic acids bearing alkyl substituents larger than a methyl group. Thus, reacting 2,6-dichloroisonicotinic acid **14** with cyclobutanolate or cyclopentanolate furnished 2-chloro-6-cyclobutoxyisonicotinic acid **15** or 2-chloro-6-cyclopentoxyisonicotinic acid **16**, respectively. Esterification using TMSCl in isopropanol to give **17** and **18** made the material ready for the following Negishi coupling. Using either dimethylzinc or diethylzinc afforded the corresponding 6-methyl or 6-ethyl-2-cycloalkoxyisonicotinates **19**, **20** and **21**, **22**, respectively. Saponification furnished the desired isonicotinic acids **12h**–**k**.

The picolinic acids **23a**–**g** required for the study of the corresponding target compounds **24a**–**g** were prepared in a similar fashion as outlined in Scheme 3. Thus, Negishi coupling of methyl 6-chloro-4-methoxypicolinate **25** using pentan-3-yl zinc bromide furnished 4-methoxy-6-(pentan-3-yl)picolinic acid as its 3-pentyl ester (**26**) in moderate yield. As observed earlier [75], the

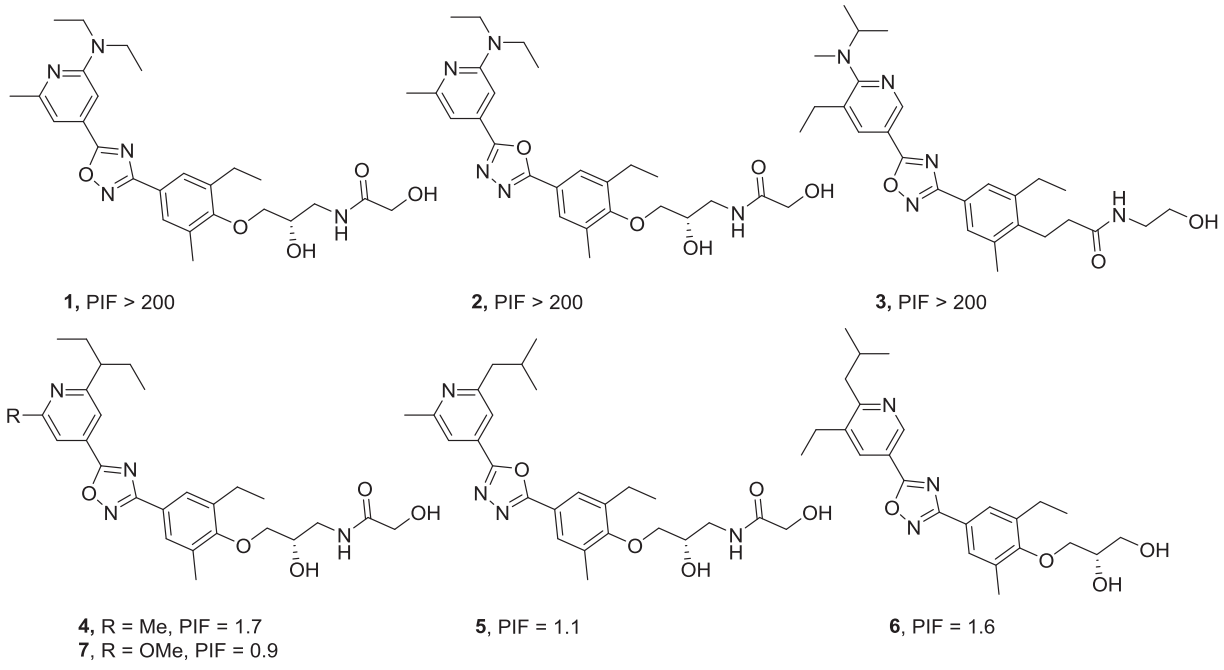

Fig. 1. Structures of the *in vitro* phototoxic aminopyridines **1**, **2**, and **3**, and the non-phototoxic alkylpyridines **4**, **5**, and **6**, and alkoxy pyridine **7a**.

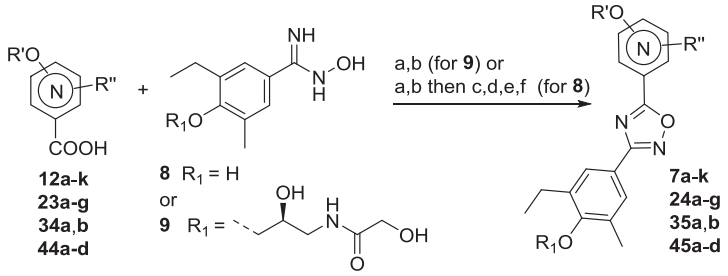

[a]Reagents and conditions: (a) TBTU, DIPEA, DCM, or THF/DMF, rt, 1 h; or HOBt, EDC HCl, THF, rt, 18 h; (b) dioxane, 80-100 °C, 7-18 h, 19-80% (2 steps); (c) (R)-glycidol, PPh_3, DEAD, THF, rt, 18 h, 76-96%, or (R)-epichlorohydrin, isopropanol, 3 N NaOH, rt, 24 h, 35-85%; (d) 7 N NH_3 in methanol, 60 °C, 18 h, 39%-quant.(crude); (e) glycolic acid, HOBt, DIPEA, EDC HCl, THF, rt, 2 h, 23-79%. For R' and R" see Tables 1 to 4.

Scheme 1. Assembling the central oxadiazole ring.[a]

$Pd(dppf)Cl_2$ catalyzed Negishi cross-coupling employing pentan-3-yl zinc bromide not only led to the formation of the picolinic acid 3-pentyl ester but also to isomerization of the 3-pentyl group attached to the pyridine. Several groups have reported on the undesired β-hydride elimination of secondary alkylzinc reagents leading to isomerized cross-coupling products and significant improvements have been achieved using further optimized catalysts, e.g. Refs. [89–91]. However, as we were able to obtain sufficient material of the desired pent-3-yl-picolinic acids **23a** and **23d** (from **31**) for our studies despite the fact that the crude reaction products contained substantial amounts of the corresponding pent-2-yl and pent-1-yl picolinic acid derivatives, we did not embark on further optimizations. β-Hydride elimination/β-migratory insertion [89] may also occur in the case of the cyclopentyl zinc reagent but as it has no consequence on the regioselectivity of the cross-coupling reaction the corresponding cyclopentyl picolinic acids **23c** and **23e** were obtained in good yield. On the other hand, $Pd(PPh_3)_4$-catalyzed cross-coupling of ethyl 6-chloro-4-methoxypicolinate **27** with 2,4,6-tris(2-methylprop-1-en-1-yl)-1,3,5,2,4,6-trioxatriborinane pyridine complex [92] furnished 4-methoxy-6-(2-methylprop-1-en-1-yl)picolinate **28** which was hydrogenated (**29**) and hydrolyzed to the desired picolinic acid **23b**. 6-(Cyclopentyloxy)-4-methylpicolinic acid **23f** was obtained in good yield by thermal displacement of the chlorine in 6-chloro-4-methylpicolinic acid **32** with cyclopentanolate. To facilitate purification, the crude product was temporarily transformed into its methyl ester. Treating the isomeric 4-chloro-6-methylpicolinic acid **33** with cyclopentanolate furnished 4-(cyclopentyloxy)-6-methylpicolinic acid **23g** in moderate yield.

The preparation of the two 5-cyclopentyl-picolinic acids **34a**

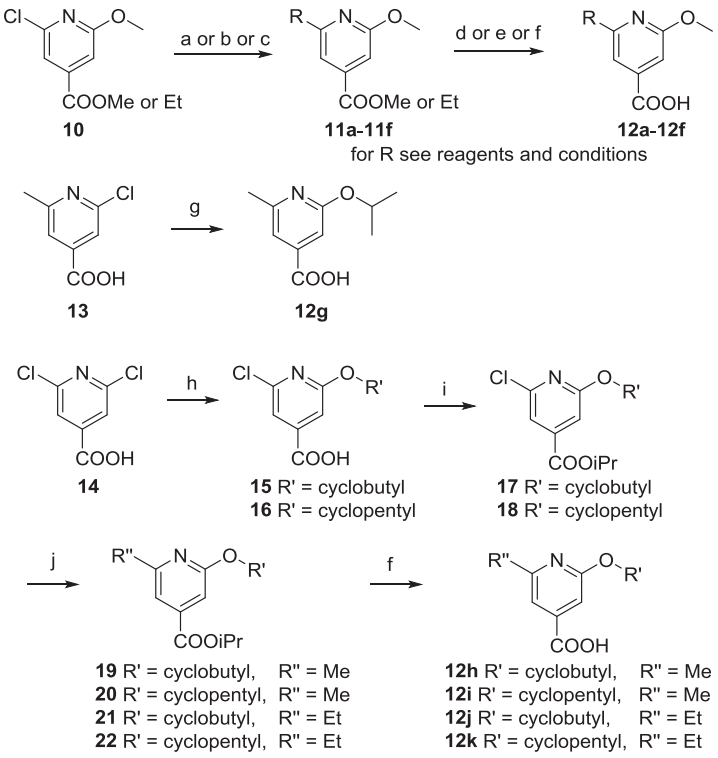

[a]Reagents and conditions: (a) alkylmagnesium bromide or chloride, $Fe(acac)_3$, THF, NMP, -75 °C 1 h, 0 °C-rt 1 h, 40-42% (R = isobutyl (**11b**)); (b) alkylzinc bromide or dialkylzinc, $Pd(dppf)Cl_2$, dioxane, 75-80 °C, 4-48 h, 50-90% (R = 3-pentyl (**11a**)), 47% (R=cyclobutyl (**11c**)), 67% (R = cyclopentyl (**11d**), 44-69% (R = cyclohexyl (**11e**)); (c) (R=Ph (**11f**)) $PhB(OH)_2$, $Pd(PPh_3)_4$, DME, 2 M aq. K_2CO_3, 80 °C, 18 h, 38%; (d) 6-7 M aq. HCl, 60-95 °C, 3-20 h, 51% (**12c**), 87-91% (**12b**), 96% - quant. (**12d**); (e) 3 M aq. NaOH, ethanol, 80°C, 2 h, 86% (**12a**); (f) 2 N aq. LiOH, THF, MeOH, or dioxane, rt, 2-18 h, 78-86% (**12e**), quant. (**12f**), 84%-quant. (**12h**), 72-88% (**12i**), quant. (**12j**), 97% (**12k**); (g) isopropanol, KOtBu, 80 °C, 72 h, 86% (**12g**); (h) cyclobutanol or cyclopentanol, NaH, dioxane, 80 °C, 24 h, 87%-quant. (crude) (**15**), quant.(crude) (**16**); (i) isopropanol, TMSCl, 50 °C, 24 h, 50-88% (**17**), 53-70% (**18**); (j) Me_2Zn (**19**, **20**) or Et_2Zn (**21**, **22**), $Pd(dppf)Cl_2$; dioxane, 75 °C, 16-24 h, 61% (**19**), 50% (**20**), 79% (**21**), 95% (**22**).

Scheme 2. Preparation of 2,6-disubstituted isonicotinic acids.[a]

and **34b** needed for the preparation of target compounds **35a** and **35b**, respectively, is summarized in Scheme 4. The synthesis of 5-cyclopentyl-4-methoxypicolinic acid **34a** started by O-alkylation of 2,5-dibromopyridin-4-ol **36** using iodomethane in the presence of K_2CO_3. Regioselective Suzuki reaction of the resulting 2,5-dibromo-4-methoxy pyridine **37** using 2,4,6-trivinyl-1,3,5,2,4,6-trioxatriborinane pyridine complex [92] delivered 5-bromo-4-methoxy-2-vinylpyridine **38** in good yield. Oxidative cleavage of the vinyl group using $KMnO_4$ established the carboxylic acid function which subsequently was converted into its methyl ester (**39**). In a second Suzuki reaction employing cyclopenten-1-yl boronic acid the carbon framework of the 5-substituent was introduced (**40**). Hydrogenation of the cyclopentene substituent (**41**) and ester cleavage afforded the desired picolinic acid **34a**. Several attempts to directly introduce the cyclopentane moiety via a Negishi reaction failed and led to decomposition of the methyl 5-bromo-4-methoxy picolinate. Commercial availability of 5-bromo-6-methoxypicolinic acid allowed for rapid access to picolinic acid **34b**. This time, $Pd(dppf)Cl_2$ catalyzed Negishi coupling of the ethyl 5-bromo-6-methoxypicolinate **42** with cyclopentyl zinc bromide afforded ethyl 5-cyclopentyl-6-methoxypicolinate **43** which upon saponification furnished the desired picolinic acid **34b**.

Finally, Scheme 5 illustrates the synthetic access to the 5,6-disubstituted nicotinic acids **44a**–**d** used to prepare the target compounds **45a**–**d**. Methyl 6-chloro-5-methoxynicotinate **46** was efficiently converted into methyl 6-cyclopentyl-5-methoxynicotinate **47** using cyclopentylmagnesium bromide under Fürstner conditions [83,84]. Subsequent ester hydrolysis

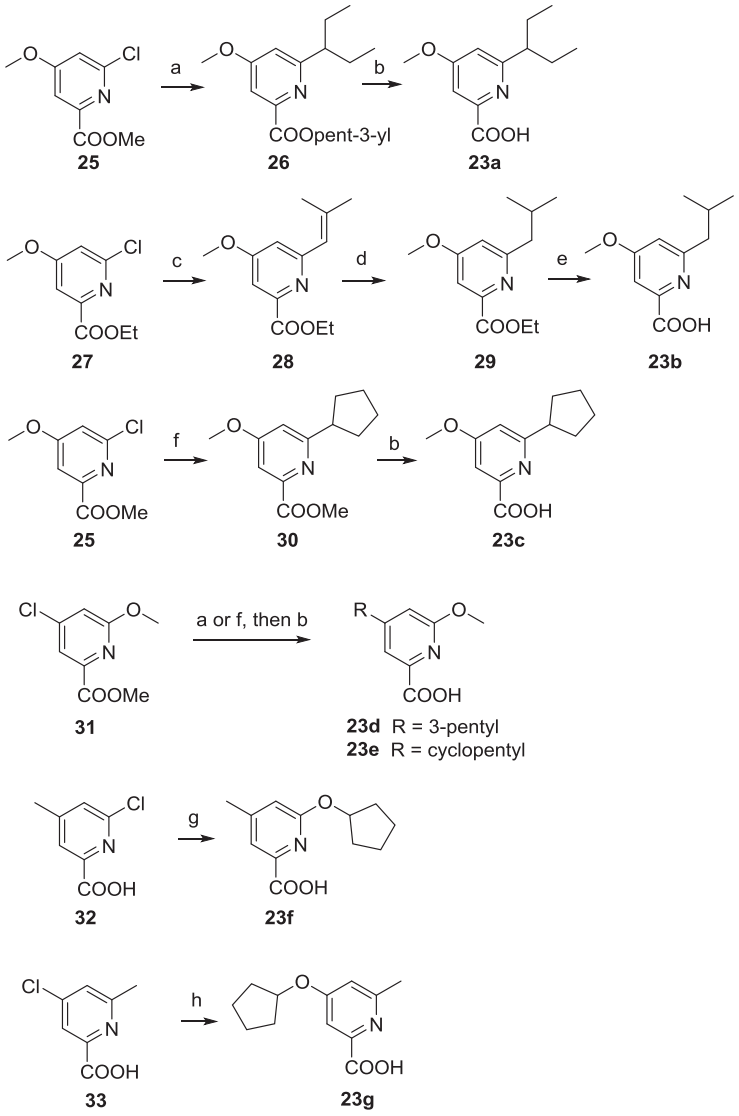

[a]Reagents and conditions: (a) pentan-3-ylzinc(II) bromide, Pd(dppf)Cl_2, dioxane, 75 °C, 18 h, 15-20% (**26**), 21% (Me ester of **23d**); (b) 2 M aq. LiOH, dioxane or methanol, rt to 75°C, 5-15 h, 98% (**23a**), 79 % (**23c**), quant. (**23d**), 88% (**23e**); (c) 2,4,6-tris(2-methylprop-1-en-1-yl)-1,3,5,2,4,6-trioxatriborinane pyridine complex, Pd(PPh_3)$_4$, DME, 100 °C, 18 h, 78% (**28**); (d) H_2, Pd/C, THF, rt, 15 h; quant. (**29**); (e) 6 N aq. HCl, 65°C, 12 h, quant. (**23b**), 84%-quant. (**23c**); (f) cyclopentylzinc(II) bromide, Pd(dppf)Cl_2, dioxane, 75 °C, 18 h, 90% (Me ester of **23e**), 50-80% (**30**); (g) (1) cyclopentanol, NaH, dioxane, 80°C, 24 h; (2) MeOH, TMSCl, 50 °C, 24 h; (3) 2 M aq. LiOH, MeOH, rt, 2 h, 84% (**23g**, 3 steps); (h) cyclopentanol, NaH, 80 °C, 24 h, 35% (**23g**).

Scheme 3. Preparation of 4,6-disubstituted picolinic acids.[a]

afforded the desired nicotinic acid **44a**. The preparation of the isomeric nicotinic acid **44c** followed a similar pathway. Thus, ethyl 5-chloro-6-methoxynicotinate **51** was coupled with cyclopenten-1-yl boronic acid to the corresponding 5-(cyclopent-1-en-1-yl)-6-methoxynicotinate **52**. Hydrogenation of the cyclopentene (**53**) followed by saponification of the nicotinic acid ester gave the desired 5-cyclopentyl-6-methoxynicotinic acid **44c**.

In the case of the 6-cyclopentoxynicotinic acid **44b**, the cyclopentoxy group was introduced by reacting 5-bromo-6-hydroxy nicotinate **48** with cyclopentanol under Mitsunobu conditions. Pd(dppf)Cl_2 catalyzed Negishi coupling of the resulting 5-bromo-6-cyclopentoxynicotinate **49** with dimethylzinc and subsequent

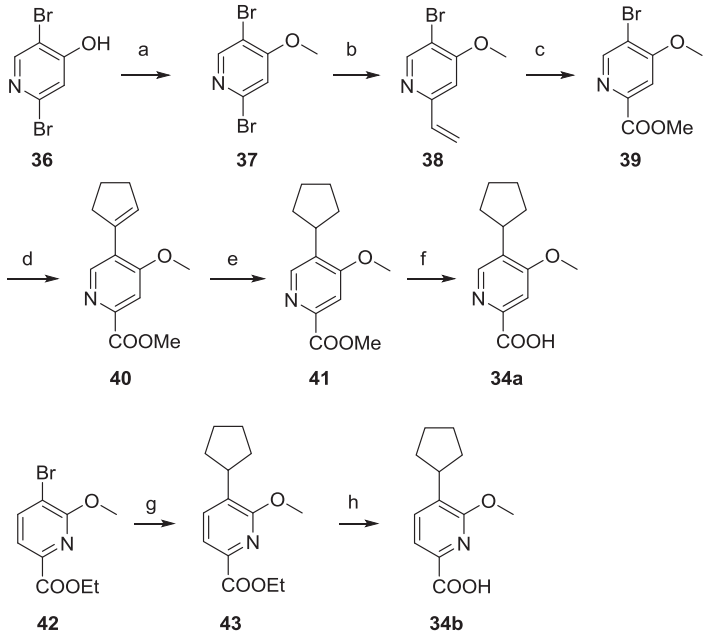

[a]Reagents and conditions: (a) MeI, K_2CO_3, DMF, 40 °C, 4 h, 35%; (b) 2,4,6-trivinyl-1,3,5,2,4,6-trioxatriborinane pyridine, $Pd(PPh_3)_4$, PPh_3, 2 M aq. K_2CO_3, dioxane, 90 °C, 3 h, 70%; (c) (1) $KMnO_4$, acetone, 0°C to rt, 16 h; (2) MeOH, H_2SO_4, 70°C, 20 h, 53% (2 steps); (d) cyclopenten-1-ylboronic acid, $Pd_2(dba)_3$, tBu_3P, Cs_2CO_3, 90 °C, 24 h, 65%; (e) H_2, Pd/C, MeOH, THF, 60 °C, 48 h, 97%; (f) 25% aq. HCl, 70°C, 16 h, 92%; (g) cyclopentylzinc(II) bromide, $Pd(dppf)Cl_2$, THF, 80 °C, 48 h, 31%; (h) MeOH, 2 M aq. LiOH, rt, 2 h, 90%.

Scheme 4. Preparation of 4,5- and 5,6-disubstituted picolinic acids.[a]

saponification afforded the desired 6-cyclopentoxynicotinic acid **44b** in good overall yield. Similarly, Mitsunobu reaction of methyl 5-hydroxy-6-iodonicotinate **54** with cyclopentanol, subsequent Negishi reaction of **55** using dimethylzinc followed by ester hydrolysis furnished the isomeric 5-cyclopentyloxy-nicotinic acid **44d**.

2.2. In vitro SAR discussion

First we explored the structure activity relationship (SAR) of 2-alkoxy substituted 4-pyridines related to compound **7a**. In a next step we extended our studies to the corresponding 2-pyridines by keeping the original meta-relationship between the alkoxy and the alkyl substituent. We then also included 2-pyridine derivatives wherein the alkoxy and the alkyl substituents were ortho to each other. Finally, the SAR studies were completed with a set of prototypical 3-pyridines. A selection of alkoxy substituted 4-, 2-, and 3-pyridines shall illustrate the SAR of the three pyridine isomer series with respect to their affinity for the $S1P_1$ and $S1P_3$ receptor, their *in vivo* efficacy as well as phototoxicity. We focus our SAR discussion on pyridine derivatives invariably incorporating the prototypical (*S*)-3-(3-ethyl-4-(2-hydroxy-3-(2-hydroxy-acetamido) propoxy)-5-methylphenyl)-1,2,4-oxadiazole moiety as this pattern usually combined high receptor affinity and *in vivo* efficacy [75,93,94]. EC_{50}-values were measured with a GTPγS binding assay using membrane preparations of CHO cells expressing either the human $S1P_1$ or $S1P_3$ receptor. Table 1 compiles a series of 4-pyridine derivatives incorporating either a small alkoxy and a large alkyl or a large alkoxy and a small alkyl substituent in position 2 and 6 of the pyridine, respectively. Both substitution patterns gave highly potent $S1PR_1$ agonists with comparable selectivities against $S1PR_3$. Specifically, the 2-methoxy-6-(3-pentyl)-pyridine **7a** showed the same affinity for $S1PR_1$ as the aminopyridine **1** and was about three times less selective against $S1PR_3$. Similarly, the isobutyl and cyclobutyl derivatives **7b** and **7c** were highly potent $S1P_1$ receptor agonists. These two compounds showed a further increased affinity for $S1PR_3$. The cyclopentyl substituted pyridine **7d** reproduced the affinity profile of the 3-pentyl analogue **7a**. On the other hand, the bulkier cyclohexyl and the phenyl substituted pyridines **7e** and **7f** both significantly lost affinity for $S1PR_1$ and $S1PR_3$. The three compounds **7g**, **7h**, and **7i** incorporating a large alkoxy substituent and a methyl group were equipotent on $S1PR_1$ and slightly more selective against $S1PR_3$ when compared to their closest analogues **7b**, **7c**, and **7d**, respectively. As illustrated with compounds **7j** and **7k** increasing the size of the alkyl substituent increased the affinity towards $S1PR_3$.

Interestingly, when the methoxy-pyridines are compared to the corresponding alkyl pyridine analogues [75], the methyl derivative reproduced the affinity profile of the methoxy compound much better than the apparently structurally closer ethyl analogue. This general finding is illustrated with the three cyclopentyl-pyridines **7d**, **7l** and **7m**. While the methoxy pyridine **7d** and methyl pyridine **7l** have an almost identical affinity profile for $S1PR_1$ and $S1PR_3$, the ethyl derivative **7m** is clearly more potent on $S1PR_3$.

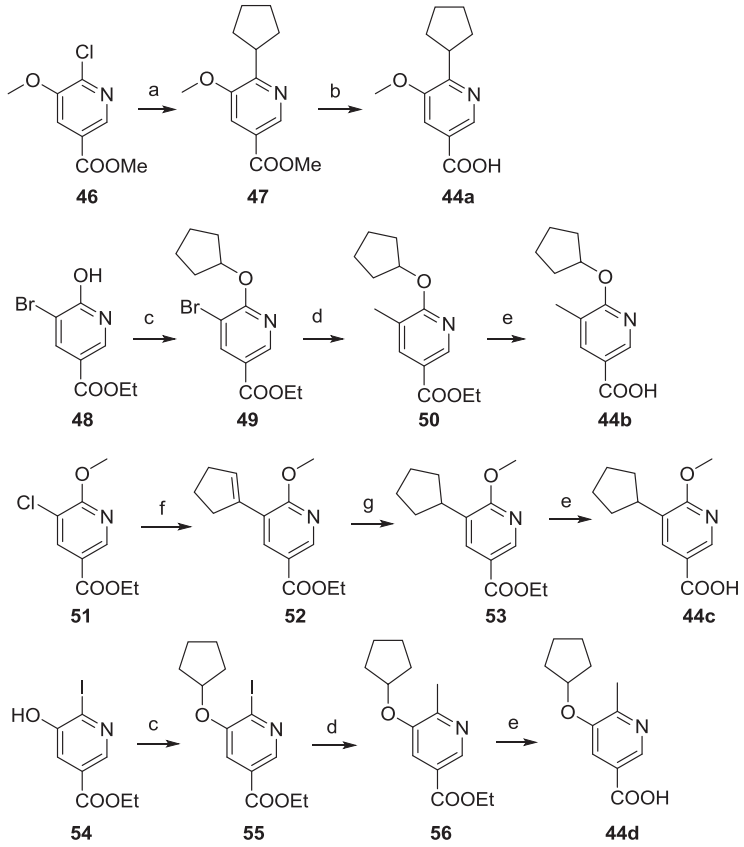

[a]Reagents and conditions: (a) cyclopentylmagnesium bromide, $Fe(acac)_3$, THF, 0 °C, 90 min, 71%, (b) 25% aq. HCl, 65 °C, 18 h, quant.; (c) cyclopentanol, PPh_3, DEAD, THF, 0-20°C, 1 h, 64-90% (**49**), 90% (**55**); (d) Me_2Zn, $Pd(dppf)Cl_2$, dioxane, 70-80 °C, 3-16 h, 58% (**50**), 68% (**56**); (e) 2 M aq. LiOH, MeOH or EtOH, rt, 2-15 h, 88% (**44b**), quant. (**44c**), 83% (**44d**); (f) cyclopenten-1-yl boronic acid, $Pd(dba)_2$, Cs_2CO_3, dioxane, 100 °C, 18 h, 27%; (g) 5 bar H_2, Pd/C, THF, EtOH, 55 °C, 48 h, 78%.

Scheme 5. Preparation of 5,6-disubstituted nicotinic acids.[a]

We then turned our attention to 2-pyridine derivatives while keeping the meta substitution pattern of the 4-pyridine series. A few examples are listed in Table 2. As in the 4-pyridine series, a 3-pentyl (**24a**), an isobutyl (**24b**), and a cyclopentyl (**24c**) substituent attached to position 6 of the 2-pyridine led to highly potent $S1PR_1$ agonists with EC_{50} values around 1 nM. However, when compared to the 4-pyridine isomers **7a**, **7b**, and **7d**, the corresponding 2-pyridines **24a**, **24b**, and **24c**, respectively, were clearly more selective against $S1PR_3$. As illustrated with compounds **24d** and **24e** swapping the positions of the methoxy and the alkyl substituent again delivered highly potent $S1PR_1$ agonists. The 3-pentyl derivative **24d** was equipotent on $S1PR_1$ but less selective against $S1PR_3$ when compared to its isomer **24a**. Conversely, the 4-cyclopentyl pyridine **24e** was less potent on both $S1PR_1$ and $S1PR_3$ than its isomer **24c**. Attaching a large alkoxy substituent to position 6 and a methyl group to position 4 (e.g. compound **24f**) reproduced the affinity profile of the 6-alkyl-4-methoxy-isomer **24c**. Interestingly, however, when the large alkoxy group was placed in position 4 and the methyl group was attached to position 6 (e.g. compound **24g**), the compound clearly lost affinity for $S1PR_1$. Two 2-pyridine derivatives wherein the substituents are ortho to each other are listed in Table 3. Interestingly, also this substitution pattern delivered highly potent $S1PR_1$ agonists and both the 4-methoxy (**35a**) and the 6-methoxy (**35b**) 5-cyclopentylpyridines showed EC_{50} values close to 1 nM. The two 4,5-disubstituted pyridines **35a** and **35b** were more potent on $S1PR_3$ when compared to their 4,6-disubstituted isomer **24c** and **24e**, respectively.

Triggered by the observation that not only 4,6- but also 4,5- and 5,6-disubstituted 2-pyridines gave highly potent $S1PR_1$ agonists, we extended our SAR studies to 5,6-disubstituted 3-pyridines. A few prototypical 3-pyridine derivatives are compiled in Table 4. Not unexpectedly, also the 3-pyridines delivered potent $S1PR_1$ agonists. The potency and selectivity profile of the 5-methoxy-6-cyclopentyl-3-pyridine **45a** was very similar to the one of the 2-pyridine isomer **35a**. Moving the oxygen from position 5 to 6 to give the 6-cyclopentoxy-5-methyl-3-pyridine **45b** had little effect on the compound's affinity towards $S1PR_1$ and $S1PR_3$. Swapping the position of the small and the large substituent in **45a** and **45b** to give the 3-pyridines **45c** and **45d** significantly increased the compounds' affinity for $S1PR_3$. On the other hand, changing the position of the oxygen in the two compounds incorporating the larger substituent in position 5 (i.e. **45c** and **45d**) clearly affected the compounds potency on $S1PR_1$.

In summary, while all pyridine series delivered potent $S1PR_1$

Table 1
SAR of 2,6-disubstituted pyridin-4-yl derivatives.

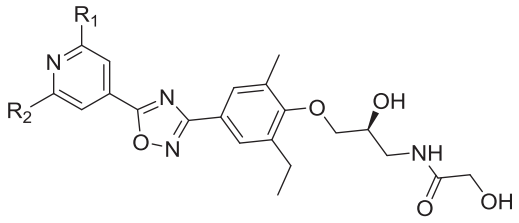

Compd	R_1	R_2	EC_{50} [nM][a]		%LC[b] (plasma conc. [nM])							DA[c] [h] (oral half-life [h])
			$S1PR_1$	$S1PR_3$	3 h	6 h	24 h	48 h	72 h	96 h	144 h	
1	Me	Diethyl-amino	0.6	350	−64	−64	−70		−62			72
7a	OMe	3-Pentyl	0.4	96	−59 (750)	−59 (470)	−36 (46)		bl[d] (<3)			6 (9)
7b	OMe	Isobutyl	0.3	27	−57	−59	−66	−59				48
7c	OMe	Cyclobutyl	0.3	22	−56	−61	−61		bl[d]			24
7d	OMe	Cyclopentyl	0.6	71	−62 (2050)	−65 (1860)	−70 (1070)			−50 (68)	−20 (12)	24 (18)
7e	OMe	Cyclohexyl	7.3	690	−58	−58	−72			−33		24
7f	OMe	Phenyl	28	1600								
7g	Isopropoxy	Me	0.2	95	−66	−67	−74			−70	−28	96
7h	Cyclobutoxy	Me	0.3	110	−66	−62	−72			−62	−21	96
7i	Cyclopentoxy	Me	1.0	190	−69 (2200)	−66 (2040)	−74 (790)		−43 (67)			24 (13)
7j	Cyclobutoxy	Et	1.1	55	−72	−75	−79					168
7k	Cyclopentoxy	Et	1.1	50	−64	−71	−76			bl[d]		24
7l[e]	Cyclopentyl	Me	0.2	47								
7m[e]	Cyclopentyl	Et	0.3	2.4								

[a] EC_{50} values as determined in a GTPγS assay using membranes of CHO cells expressing either $S1PR_1$ or $S1PR_3$ [95]; EC_{50} values represent the geometric mean of at least three independent measurements.
[b] %Lymphocyte count reduction at indicated time point post oral administration of 10 mg/kg of compound as compared to baseline values, plasma concentrations given in brackets, limit of quantification = 3 nM.
[c] DA [h] = duration of maximal LC reduction as defined by the latest time point at which maximal LC reduction was observed.
[d] bl = LC reached baseline value.
[e] Data from Ref. [75].

Table 2
SAR of 4,6-disubstituted pyridin-2-yl derivatives.

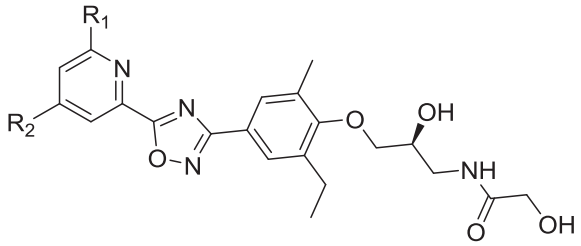

Compd	R_1	R_2	EC_{50} [nM][a]		%LC[b] (plasma conc. [nM])			DA[c] [h] (oral half-life [h])
			$S1PR_1$	$S1PR_3$	3 h	6 h	24 h	
24a	3-Pentyl	OMe	1.2	520				
24b	Isobutyl	OMe	1.5	1400	−58	−66	−23	6
24c	Cyclopentyl	OMe	0.7	800	−58	−61	−30	6
24d	OMe	3-Pentyl	1.1	180	−57 (410)	−50 (240)	10 (12)	<3[d](4)
24e	OMe	Cyclopentyl	4.5	1500	−63 (1790)	−75 (1300)	2 (100)	6 (5)
24f	Cyclopentoxy	Me	1.0	930	−51 (1610)	−58 (890)	18 (39)	6 (4)
24g	Me	Cyclopentoxy	11	1400	−50 (1560)	−36 (510)	33 (<9)	<3[d] (<3)

[a,b,c]See caption Table 1.
[d]Maximal LC reduction not reached.

agonists, there are clear differences between the SAR of the individual isomer series. For instance, while a cyclopentoxy substituent gave highly potent compounds in the 4-pyridine series and when placed position 6 in the 2-pyridine series, it clearly hampered the affinity for $S1PR_1$ in position 4 of the 2-pyridine. In addition, the cyclopentyl substituted 4-pyridine **7d** and the corresponding 3-pyridine **45c** both showed an EC_{50} value of about 1 nM on $S1PR_1$, while performing the same structural modification in going from the cyclopentoxy substituted 4-pyridine **7i** to the corresponding 3-pyridine analogue **45d** led to a clear loss in affinity for $S1PR_1$. (Note that for the first pair (**7d**, **45c**), the nature of the pyridine remains an 'O-alkylated 2-pyridone', while for the second pair (**7i**, **45d**), the

Table 3
SAR of 4,5- and 5,6-di-substituted pyridin-2-yl derivatives.4

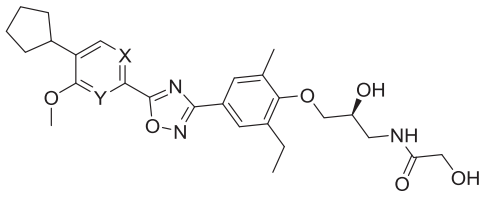

Compd	X	Y	EC_{50} [nM][a]		%LC[b] (plasma conc. [nM])			DA[c] [h] (oral half-life [h])
			$S1PR_1$	$S1PR_3$	3 h	6 h	24 h	
35a	N	CH	0.6	210	−79 (2520)	−86 (2020)	−60 (71)	6 (4)
35b	CH	N	1.4	920	−70 (690)	−78 (500)	−23 (61)	6 (6)

[a,b,c]See caption Table 1; additional time point: %LC(plasma conc.): **35a** 72 h: back to baseline (<3 nM).

Table 4
SAR of 5,6-disubstituted pyridin-3-yl derivatives.5

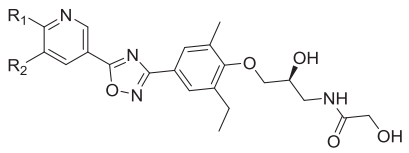

Compd	R_1	R_2	EC_{50} [nM][a]		%LC[b] (plasma conc. [nM])			DA[c] [h] (oral half-life [h])
			$S1PR_1$	$S1PR_3$	3 h	6 h	24 h	
45a	Cyclopentyl	OMe	0.3	71	−73 (2390)	−82 (2950)	−84 (970)	24 (11)
45b	Cyclopentoxy	Me	0.7	140	−76 (1140)	−85 (960)	−85 (510)	24 (16)
45c	OMe	Cyclopentyl	1.5	17				
45d	Me	Cyclopentoxy	21	38				

[a,b,c]See caption Table 1; additional time points: %LC (plasma conc.): **45a** 96 h: back to baseline (<10 nM); **45b** 72 h: −32% (58 nM), 144 h: back to baseline (<3 nM).

nature of the pyridine changes from an 'O-alkylated 2-pyridone' to a '3-alkoxy-pyridine'.) Interestingly, in both cases the affinity for $S1PR_3$ increases by a factor of 4–5. These observations clearly indicate that steric and electronic factors contribute to the ligand receptor binding interaction.

2.3. *In vivo efficacy assessment*

For prototypical compounds (usually with an EC_{50} ≤10 nM on $S1PR_1$) the efficacy to reduce the peripheral blood lymphocyte count (LC) was assessed in the rat. The compounds were administered orally at a dose of 10 mg/kg to male Wistar rats and blood LC was measured shortly before and 3, 6, and 24 h after compound administration. For several compounds later sampling time points were added to confirm complete recovery of the LC. Due to significant inter-individual variability and the circadian rhythm of the absolute number of circulating lymphocytes, a LC change of ±15% was considered to be within baseline. On the other hand, a LC reduction of ≥60% was interpreted as the maximal effect that is achieved under the experimental conditions chosen [95]. The duration of action (DA) was defined as the latest time point at which maximal LC reduction was observed. For about half of the compounds tested *in vivo*, plasma concentrations reached in the LC experiment were measured and oral half-lives were calculated based on these exposure data. Values for the measured LC and plasma concentrations, and estimated DA and oral half-lives are given in Tables 1–4. In line with what is reported for $S1PR_1$ agonists [24,25,44,54,58], our pyridine derivatives reduced the LC in a rapid and reversible fashion. In general, compounds with an EC_{50} <5 nM on $S1PR_1$ showed *in vivo* efficacy.

All 4-pyridines tested *in vivo* showed a rapid onset of action and the LC was maximally reduced at 3 h post administration already (Table 1). In addition, these compounds showed a DA of at least 24 h. The cyclopentyl pyridine **7d** and the cyclopentoxy pyridine **7i** showed micromolar plasma concentrations over 24 h, suggesting that the 4-pyridines were well absorbed and slowly cleared. Oral half-lifes of **7d** and **7i** were 13 and 18 h, respectively. The 3-pentyl substituted pyridine **7a** showed a DA of less than 24 h. In agreement with earlier observations [75], and as demonstrated by the plasma concentrations and the oral half-life the 3-pentyl pyridine **7a** was more rapidly cleared than its cyclopentyl analogue **7d**. As a consequence the LC already partially recovered at 24 h.

Interestingly, even though the 2-pyridines listed in Table 2 showed similar potencies when compared to the corresponding 4-pyridine analogues, they clearly displayed a different behaviour *in vivo*. The duration of action of the 2-pyridines was consistently shorter (e.g. compare **24b** with **7b**, **24c** with **7d**, **24g** and **24f** with **7i**) and at a dose of 10 mg/kg none of the tested 2-pyridines produced a maximal LC reduction for 24 h. Plasma concentrations at 3 h were comparable to those reached with the corresponding 4-pyridines but dropped much more rapidly at 6 and, in particular, 24 h (compare e.g. **24f** and **24g** with **7i**, and **24e** with **7d**) translating into rather short oral half-lifes of 3–5 h. The 4,5- and 5,6-disubstituted 2-pyridines in Table 3 showed a very similar *in vivo* behaviour. Also here, plasma concentrations were high at 3 h post administration but dropped significantly at 24 h. With 4 and 6 h, respectively, the oral half-life of compounds **35a** and **35b** was too short to maintain maximal LC reduction over 24 h.

On the other hand, the two 3-pyridines **45a** and **45b** (Table 4) exhibited pharmacokinetic and pharmacodynamic profiles comparable to those of the corresponding 4 pyridines **7d** and **7i**, respectively. Both compounds sustained rather high plasma concentrations over 24 h and as a consequence showed maximal LC reduction for at least 24 h.

Hence, the PK and PD data suggest that the nature of the pyridine isomer rather than the substitution pattern governs the pharmacokinetic behaviour of the compound. The oral half life for the 2-, 3-, and 4-pyridines was estimated to be 3–6 h, 11–16 h, and 13–18 h, respectively. Clearance and compound tissue distribution (Vss) determine the half-life of a compound *in vivo*. To rationalize the above PK observations, we predicted the Vss values for the compounds tested *in vivo* using a rat physiology based pharmacokinetic model using GastroPlus. The predicted values for Vss were in the range of 0.8–1.5 L/kg for all three pyridine isomer classes suggesting that the observed differences in half-life are largely driven by differences in the clearance of the compounds.

2.4. In vitro phototoxicity assessment

As mentioned in the introduction, the observation that compound **7a** was not *in vitro* phototoxic (PIF = 0.9) triggered a more detailed investigation whether alkoxy substituted pyridine derivatives would serve as potent and efficacious $S1P_1$ receptor agonists. As a first step to assess the phototoxic potential of these compounds, UV spectra of prototypical representatives of each pyridine isomer series were measured. While all compounds showed an absorption maximum at around 254 nm, some showed a second absorption maximum at wavelengths >290 nm. However, as the molar extinction at wavelengths ≥290 nm of all compounds – including **7a** – were in a range (ε >1000) where the guidelines [80,81] recommend a more detailed phototoxicity assessment, the *in vitro* photo-irritancy factor (PIF) of these compounds was determined using the Balb/c mouse 3T3 fibroblast neutral red uptake assay [76,77]. Table 5 compiles the obtained PIF values and the molar extinction coefficient at the absorbance maximum at >290 nm. In case the UV spectrum showed no absorption maximum at wavelengths >290 nm, the molar extinction at 290 nm is given.

Compared to aminopyridine **1**, the PIF values of the alkoxy pyridines listed in Table 5 are much smaller. In fact, we consider compounds **7a**, **7d**, **24c**, **24e**, **24f**, **24g**, **35a**, and **45b** to be non-phototoxic *in vitro*. In contrast, with a PIF value in the range of 6.5–7.5 the pyridines **7i**, **35b**, and **45a** showed clear sign of *in vitro* phototoxicity. These three compounds showed strong light absorption at wavelengths >290 nm (ε >10 000). Despite showing a similarly high extinction (ε >10 000) at the second λ_{max} compounds **24f**, **35a** and **45b** were not phototoxic. Interestingly, for **35a** and **45b** the second absorption maximum occurred at wavelengths below 290 nm. This observation prompted us to revisit the technical details of the 3T3 fibroblast phototoxicity assay. As recommended by the guidelines, and due to the UVB sensitivity of the Balb/c 3T3 cell line, the light filter used in the mouse 3T3 fibroblast phototoxicity assay completely blocks light transmission at wavelengths ≤300 nm. While some transmission occurs at 310 nm, significant exposure is obtained above 320 nm only (for details see Supporting information). We therefore calculated the area under the curve (AUC) of the UV spectra between 310 and 350 nm (highest wavelength at which light absorption was observed) normalized to the compound concentration in μM. As shown by the results given in Table 5, the normalized AUC values indeed correlate with the compound's phototoxic potential. Compound **1** showing the highest PIF value also reached the highest AUC value (0.54). The three phototoxic alkoxy pyridines **7i**, **35b**, and **45a** had smaller AUC values than **1** but scored highest when compared to the remaining, non-phototoxic alkoxy pyridines. The threshold for the AUC to observe *in vitro* phototoxicity appears to be around 0.10 OD nm/μM. Whether this threshold is characteristic for the alkoxy-pyridine series of the present study or could also be applied to other compound series is not known and additional studies extending the concept of integrating UV spectra to better predict *in vitro* phototoxicity of other compound classes are certainly warranted.

The above considerations clearly confirm that the UV absorption correlates with the phototoxic potential of a compound. However, it was much more difficult to establish a direct structure phototoxicity relationship. By analyzing the UV spectra in more detail, a few structural elements that affect the compound's UV spectrum and hence its behaviour in the phototoxicity assay could be identified and are discussed below. While all compounds showed a first absorption maximum between 249 and 264 nm, the 4-pyridines (**7a**, **7d**, **7i**), the 3-pyridines (**45a**, **45b**) and the 2-pyridine (**35b**) bearing the alkoxy substituent ortho to the pyridine nitrogen had a second absorption maximum above 290 nm. In contrast, the 2-pyridines wherein the alkoxy substituent is attached in para to the nitrogen (**24a** (see Supporting information), **24c**, **24g**, **35a**) show no second absorption maximum. While the molar extinction at 290 nm of these four 4-alkoxy-2-pyridines ranged from 4600 to 11800, their

Table 5
Photo-irritancy factor (PIF) values of prototypical compounds of each pyridine isomer series.[a]

Compound	Molar extinction coefficient (ε) at λ_{max} >290 nm (λ_{max} [nm])	$AUC_{310-350\ nm}$ [b] [OD nm/μM]	PIF value
1	2000 (380)[c]	0.54[d]	>200[e]
7a	2200 (310)	0.05	0.9
7d	4300 (311)	0.09	2.3
7i	18,100 (296)	0.12	7.5
24c	4600[f]	0	2.4
24e	3700 (313)	0.09	2.1
24f	12,500 (301)	0.10	2.0
24g	6300[f]	0	1.3
35a	11,800[f]	0.02	2.1
35b	18,800 (302)	0.17	6.5
45a	14,000 (302)	0.15	7.6
45b	23,700[f]	0.02	1.4

[a] As measured in the mouse 3T3 fibroblast neutral red uptake assay; for details see Supporting information.
[b] AUC of the UV spectra between 310 and 350 nm normalized to compound concentration in μM.
[c] Compound is fluorescent.
[d] $AUC_{310-435\ nm}$ as absorption extends to 435 nm.
[e] Please note that compound **1** did not degrade in the course of the *in vitro* phototoxicity assay.
[f] No absorption maximum at wavelengths >290 nm, extinction at 290 nm given.

$AUC_{310-350nm}$ value is small (0–0.02) and none of the compounds was phototoxic *in vitro*. For the compounds showing a second absorption maximum >290 nm, the size of the alkyl group attached to the oxygen appears to influence the compound's UV-absorption. When a cyclopentyl rather than a methyl group was attached to the oxygen the compound absorbed more UV light at wavelengths >290 nm (compare e.g. **24e** with **24f**, and **7d** with **7i**). While UV absorption of the 2-cyclopentyl-6-methoxy pyridine **7a** is not sufficient to induce *in vitro* phototoxicity, the one of the isomeric 2-methyl-6-cyclopentoxy pyridine **7i** is obviously strong enough to trigger a clear phototoxicity signal. Unfortunately, a more detailed correlation between structure and UV spectrum remained elusive at this point.

In brief, the majority of the alkoxy pyridine isomers are not phototoxic. In addition, the PIF value of those compounds that did show *in vitro* phototoxicity is much lower compared to the one of the aminopyridine **1**. Furthermore, while the maximal extinction at wavelengths ≥290 nm serves as an easy and rapidly available basis for the decision whether the phototoxic potential of a compound needs to be assessed in detail, the somewhat more sophisticated concentration normalized integration of a compound's UV/VIS spectrum may be more suitable to predict and rationalize the results of the *in vitro* phototoxicity assay.

3. Conclusions

In summary, starting from the phototoxic aminopyridine **1** we identified a series of alkoxy substituted 2-, 3-, and 4-pyridine analogues with no or a significantly reduced phototoxic potential. While all three alkoxy pyridine isomer series showed similarly high activity on the $S1P_1$ receptor, their selectivity against the $S1P_3$ receptor and their *in vivo* efficacy differed significantly. The 2-pyridines were clearly more selective against $S1PR_3$ when compared to the corresponding 3- or 4-pyridine analogues (e.g. compare **35a** vs **45a**, **24c** and **24e** vs **7d**). Interestingly, despite having a different substitution pattern at the pyridine ring, the selectivity profile of the 3-pyridines was almost identical to the one of the 4-pyridines (e.g. compare **45a** vs **7d**, **45b** vs **7i**). On the other hand, the oral half-life and as a consequence the pharmacological duration of action after oral administration of the 2-pyridines was significantly shorter when compared to the corresponding 3- or 4-pyridines. This indicates that the position of the pyridine nitrogen relative to the oxadiazole rather than the position of the alkyl and alkoxy substituents governs the pharmacokinetic behaviour of the compound. With respect to their potency and selectivity profile and their *in vivo* efficacy, the 2-pyridine **24c**, the 3-pyridine **45b**, and the 4-pyridine **7d** are the best representatives of each pyridine isomer series. None of these three compounds was phototoxic in the 3T3 mouse fibroblast neutral red uptake assay. Compound **45b**, in particular, incorporates an attractive combination of a long duration of action *in vivo* and a high selectivity against $S1PR_3$. At this point more detailed profiling and careful assessment of the importance of the different properties of these compounds is needed to judge their potential for human use.

4. Experimental section

4.1. Syntheses

All reagents and solvents were used as purchased from commercial sources (Sigma–Aldrich Switzerland, Lancaster Synthesis GmbH, Germany, Acros Organics USA). Moisture sensitive reactions were carried out under an argon atmosphere. Progress of the reactions was followed either by thin-layer chromatography (TLC) analysis (Merck, 0.2 mm silica gel 60 F_{254} on glass plates) or by LC–MS. **LC–MS**: Finnigan MSQ™ plus or MSQ™ surveyor (Dionex, Switzerland), with HP 1100 Binary Pump and DAD (Agilent, Switzerland), column: Zorbax SB-AQ, 5 μm, 120 Å, 4.6 × 50 mm (Agilent), or (LC–MS*) Zorbax SB-AQ, 5 μm, 120 Å, 4.6 × 20 mm (Agilent); gradient: 5–95% acetonitrile in water containing 0.04% of trifluoroacetic acid, within 1 min, flow: 4.5 mL/min; t_R is given in min. *denotes basic conditions: gradient: 5–95% acetonitrile in water containing 0.04% of ammonium hydroxide, within 1 min, flow: 4.5 mL/min. Purity of all target compounds was confirmed by a second, independent LC–MS method (LC–MS**) on a Waters Acquity UPLC system equipped with an ACQ-PDA detector, an ACQ-ESL detector, and an ACQ-SQ detector; column: ACQUITY UPLC BEH C18 1.7 μm, 2.1 × 50 mm; gradient: 2–98% acetonitrile containing 0.045% formic acid in water containing 0.05% formic acid over 1.8 min; flow 1.2 mL/min; 60 °C. According to the LC–MS analyses, target compounds showed a purity >95% (UV at 211–214 nm). Purity and identity were further corroborated by **LC-HRMS**: Analytical pump: Waters Acquity Binary, Solvent Manager, MS: SYNAPT G2 MS, source temperature: 150 °C, desolvation temperature: 400 °C, desolvation gas flow: 400 L/h; cone gas flow: 10 L/h, extraction cone: 4 RF; lens: 0.1 V; sampling cone: 30; capillary:1.5 kV; high resolution mode; gain: 1.0, MS function: 0.2 s per scan, 120–1000 amu in full scan, centroid mode. Lock spray: Leucine enkephalin 2 ng/mL (556.2771 Da) scan time 0.2 s with interval of 10 s and average of 5 scans; DAD: Acquity UPLC PDA Detector. Column: Acquity UPLC BEH C18 1.7 μm 2.1 × 50 mm from Waters, thermostated in the Acquity UPLC Column Manager at 60 °C. Eluents: water +0.05% formic acid; B: acetonitrile +0.05% formic acid. Gradient: 2–98% B over 3.0 min. Flow: 0.6 mL/min. Detection: UV 214 nm and MS, t_R is given in min; and by **NMR spectroscopy**: (Bruker Avance II, 400 MHz UltraShield™, 400 MHz (^{1}H), 100 MHz (^{13}C); or Bruker Avance III HD, Ascend 500 MHz (^{1}H), 125 MHz (^{13}C) magnet equipped with DCH cryoprobe), chemical shifts are reported in parts per million (ppm) relative to tetramethylsilane (TMS), and multiplicities are given as s (singlet), d (doublet), t (triplet), q (quartet), quint (quintuplet), h (hextet), hept (heptuplet) or m (multiplet), br = broad, coupling constants are given in Hz). Compounds were purified by either flash **column chromatography** (CC) on silica gel 60 (Fluka Sigma–Aldrich, Switzerland), prep. **TLC** glass plates coated with silica gel 60 F_{254} (0.5 mm), or by **prep. HPLC** (Waters XBridge™ Prep C18, 5 μm, OBD, 19 × 50 mm, or Waters X-terra™ RP18, 19 × 50 mm, 5 μm, gradient of acetonitrile in water containing 0.4% of formic acid, flow 75 mL/min), or by **MPLC** (Labomatic MD-80-100 pump, Linear UVIS-201 detector, column: 350 × 18 mm, Labogel-RP-18-5s-100, gradient: 10% methanol in water to 100% methanol). **UV-spectra** were acquired on a Varian Cary 50 Scan UV/Vis Spectrometer with Varian UV Scan Software Version 3.0 and Cary Win UV Kinetics Application Software Version 3.0.

4.1.1. Preparation of pyridine carboxylic acid building blocks

4.1.1.1. 2-Methoxy-6-(pentan-3-yl)isonicotinic acid (*12a*)

(a) Under argon, Pd(dppf) (3.04 g, 4 mmol) was added to a solution of 2-chloro-6-methoxy-isonicotinic acid methyl ester (50 g, 0.248 mol) in THF (100 mL). A 0.5 M solution of 3-pentylzincbromide in THF (550 mL) was added via dropping funnel. Upon complete addition, the mixture was heated to 85 °C for 18 h before it was cooled to rt. Water (5 mL) was added and the mixture is concentrated. The crude product was purified by filtration over silica gel (350 g) using heptane:EA 7:3 to give methyl 2-methoxy-6-(pentan-3-yl)-isonicotinate **11a** (53 g, 90%) as a pale yellow oil; LC–MS: $t_R = 0.99$ min, $[M + 1]^+ = 238.32$; ^{1}H NMR ($CDCl_3$): δ 7.23 (s,

1H), 7.12 (d, J = 0.6 Hz, 1H), 3.96 (s, 3H), 3.95 (s, 3H), 2.48–2.56 (m, 1H), 1.64–1.82 (m, 4H), 0.79 (t, J = 7.4 Hz, 6H).

(b) A solution of methyl 2-methoxy-6-(pentan-3-yl)isonicotinate **11a** (50 g, 211 mmol) in water (50 mL), 32% aq. NaOH (50 mL) and ethanol (250 mL) was stirred at 80 °C for 2 h. The mixture was concentrated, diluted with water and extracted with tert-butyl methyl ether (TBME). The aqueous phase was acidified by adding 25% aq. HCl and then extracted twice with EA (2 × 400 mL). The organic extract was concentrated and the residue was precipitated from water (550 mL). The product was collected, dried under high vacuum to give the title compound (40.2 g, 86%) as a white powder; LC–MS: t_R = 0.85 min, $[M + 1]^+$ = 224.37; ^{1}H NMR (DMSO-d_6): δ 7.20 (s, 1H), 7.00 (s, 1H), 3.88 (s, 3H), 2.53–2.59 (m, 1H), 1.58–1.74 (m, 4H), 0.74 (t, J = 7.2 Hz, 6H).

4.1.1.2. 2-Isobutyl-6-methoxyisonicotinic acid (**12b**)

(a) Under argon, to a solution of ethyl 2-chloro-6-methoxyisonicotinate **10** (3.53 g, 16.4 mmol) in THF (50 mL) was added Fe(acac)$_3$ (636 mg, 1.80 mmol) followed by NMP (2.27 g, 22.9 mmol). The mixture was cooled to −75 °C before isobutylmagnesium chloride (13 mL of a 2 M solution in THF) was added. The mixture was stirred at −75 °C for 1 h, then at 0 °C for 1 h. The reaction was quenched by carefully adding water (100 mL) and the mixture was extracted with diethyl ether. The organic extract was dried over $MgSO_4$, filtered and concentrated. The crude product was purified by CC on silica gel eluting with heptane:EA 9:1 to give ethyl 2-isobutyl-6-methoxyisonicotinate **11b** (1.54 g, 40%) as a pale yellow oil; LC–MS: t_R = 1.06 min, $[M + 1]^+$ = 238.13.

(b) A solution of ethyl 2-isobutyl-6-methoxyisonicotinate **11b** (1.53 g, 6.45 mmol) in 25% aq. HCl (20 mL) was stirred at 70 °C for 5 h. The solvent was removed in vacuo and the remaining residue was dried under HV to give the still water containing hydrochloride salt of the title compound (1.45 g, quant.) as a pale yellow solid; LC–MS: t_R = 0.87 min, $[M + 1]^+$ = 210.09; ^{1}H NMR (DMSO-d_6): δ 7.21 (s, 1H), 7.00 (s, 1H), 4.37 (s br, 2H + H_2O), 3.87 (s, 3H), 2.58 (d, J = 7.1 Hz, 2H), 1.99–2.13 (m, 1H), 0.88 (d, J = 6.7 Hz, 6H).

4.1.1.3. 6-Cyclopentoxy-5-methyl-nicotinic acid (**44b**)

(a) A suspension of 5-bromo-6-hydroxy nicotinic acid (5.00 g, 22.9 mmol) in ethanol (200 mL) and H_2SO_4 (0.5 mL) was stirred at 90 °C for 18 h. The solid dissolves slowly. The mixture was concentrated and the residue was dissolved in EA and washed with water. The washing was extracted back once with DCM. The combined organic extracts were dried over $MgSO_4$, filtered and concentrated to give ethyl 5-bromo-6-hydroxy nicotinate **48** (5.13 g, 91%) as a pale yellow oil; LC–MS: t_R = 0.72 min; $[M + 1]^+$ = 245.87.

(b) To a solution of ethyl 5-bromo-6-hydroxy nicotinate **48** (5.10 g, 20.7 mmol) in THF (150 mL) triphenylphosphine (8.16 g, 31.1 mmol) and cyclopentanol (2.14 g, 24.9 mmol) was added. The mixture was cooled to 0 °C before diethyl azodicarboxylate (14.2 mL, 40% solution in toluene) was slowly added. Upon completion of the addition, the green mixture was stirred at 10 °C for 30 min before it was diluted with EA and washed with water and brine. The organic extract was dried over $MgSO_4$, filtered and concentrated. The crude product was purified by CC on silica gel eluting with heptane:EA 9:1 to give ethyl 5-bromo-6-(cyclopentyloxy) nicotinate **49** (5.87 g, 90%) as a colourless oil; LC–MS: t_R = 1.12 min; $[M + 1]^+$ = 315.85.

(c) To a solution of ethyl 5-bromo-6-(cyclopentyloxy)nicotinate **49** (2.00 g, 6.37 mmol) in dioxane (100 mL) under argon, Pd(dppf) (104 mg, 0.127 mmol) and dimethylzinc (6.5 mL of a 1.2 M solution in toluene) was added. The mixture was stirred at 80 °C for 3 h. The mixture was cooled to rt and the reaction was quenched by adding water. The mixture was extracted with EA. The organic extract was washed with water, dried over $MgSO_4$, filtered and concentrated. The crude product was purified by CC on silica gel eluting with heptane:EA 9:1 to give ethyl 6-(cyclopentyloxy)-5-methylnicotinate **50** (920 mg, 58%) as a colourless oil; LC–MS: t_R = 1.09 min; $[M + 1]^+$ = 250.05.

(d) A solution of ethyl 6-(cyclopentyloxy)-5-methylnicotinate **50** (920 mg, 3.69 mmol) in ethanol (10 mL) and 1 M aq. NaOH (2 mL) was stirred at rt for 2 h. The mixture was acidified by adding 1 N aq. HCl (5 mL) and extracted twice with EA. The combined organic extracts were dried over $MgSO_4$, filtered, concentrated and dried under high vacuum to give the title compound (720 mg, 88%) as a white solid; LC–MS: t_R = 0.92 min; $[M + 1]^+$ = 222.01; ^{1}H NMR ($CDCl_3$): δ 8.78 (d, J = 1.7 Hz, 1H), 8.01 (s br, 1H), 5.55–5.60 (m, 1H), 2.21 (s, 3H), 1.95–2.08 (m, 2H), 1.77–1.90 (m, 4H), 1.62–1.73 (m, 2H).

4.1.2. Method A: Preparation of target compounds starting from hydroxy-amidine **9**

*4.1.2.1. N-[(S)-3-(2-Ethyl-4-{5-[2-(1-ethyl-propyl)-6-methoxy-pyridin-4-yl]-1,2,4-oxadiazol-3-yl}-6-methyl-phenoxy)-2-hydroxy-propyl]-2-hydroxy-acetamide (**7a**).* To a solution of 2-methoxy-6-(pentan-3-yl)isonicotinic acid hydrochloride **12a** (200 mg, 0.77 mmol) in DMF (3 mL) and THF (10 mL), DIPEA (200 mg, 1.54 mmol) followed by TBTU (272 mg, 0.847 mmol) was added. The mixture was stirred at rt for 10 min before *N*-((*S*)-3-[2-ethyl-4-(*N*-hydroxycarbamimidoyl)-6-methyl-phenoxy]-2-hydroxy-propyl)-2-hydroxy-acetamide **9** [75,96] (251 mg, 0.77 mmol) was added. Stirring was continued for 30 min. The mixture was diluted with EA (100 mL) and washed with brine. The organic extract was concentrated and the residue was dissolved in dioxane (50 mL). The mixture was stirred at 100 °C for 2 h before it was concentrated. The crude product was purified on prep. TLC plates using DCM:MeOH 10:1 to give the title compound (180 mg, 46%) as a colourless foam; LC–MS**: t_R = 1.49 min, $[M + 1]^+$ = 513.4; ^{1}H NMR ($CDCl_3$): δ 7.88 (s, 1H), 7.86 (s, 1H), 7.43 (d, J = 1.1 Hz, 1H), 7.31 (d, J = 1.1 Hz, 1H), 7.09 (s br, 1H), 4.18–4.25 (m, 3H), 4.01 (s, 3H), 3.75–3.93 (m, 4H), 3.50–3.59 (m, 1H), 2.74 (q, J = 7.5 Hz, 2H), 2.54–2.64 (m, 1H), 2.38 (s, 3H), 1.65–1.89 (m, 4H), 1.31 (t, J = 7.5 Hz, 3H), 0.84 (t, J = 7.4 Hz, 6H); ^{13}C NMR ($CDCl_3$): δ 174.4, 173.4, 168.9, 165.1, 164.5, 157.3, 137.7, 133.4, 131.6, 128.4, 126.7, 122.6, 113.5, 106.1, 74.1, 70.2, 62.2, 53.7, 51.2, 42.3, 27.9, 22.9, 16.5, 14.8, 12.2; LC-HRMS: t_R = 1.58 min, $[M + H]/z$ = 513.2713 ($C_{27}H_{37}N_4O_6$), found = 513.2711; UV(MeOH): 249(31800), 310(2200), ε_{290}(1800).

*4.1.2.2. N-((S)-3-{4-[5-(6-Cyclopentyl-4-methoxy-pyridin-2-yl)-1,2,4-oxadiazol-3-yl]-2-ethyl-6-methyl-phenoxy}-2-hydroxy-propyl)-2-hydroxy-acetamide (**24c**).* Method A, 57%, pale yellow resin; LC–MS**: t_R = 1.28 min, $[M + 1]^+$ = 511.3; ^{1}H NMR ($CDCl_3$): δ 7.92

(s, 1H), 7.91 (s, 1H), 7.69 (d, $J = 2.3$ Hz, 1H), 7.03 (t br, $J = 5.6$ Hz, 1H), 6.94 (d, $J = 2.3$ Hz, 1H), 4.19–4.24 (m, 3H), 3.99 (s, 3H), 3.90 (dd, $J_1 = 4.7$ Hz, $J_2 = 9.6$ Hz, 1H), 3.84 (dd, $J_1 = 6.3$ Hz, $J_2 = 9.5$ Hz, 1H), 3.80 (ddd, $J_1 = 3.2$ Hz, $J_2 = 6.7$ Hz, $J_3 = 14.2$ Hz, 1H), 3.49–3.56 (m, 1H), 3.32–3.40 (m, 1H), 2.74 (q, $J = 7.6$ Hz, 2H), 2.38 (s, 3H), 2.16–2.24 (m, 2H), 1.71–1.93 (m, 6H), 1.32 (t, $J = 7.6$ Hz, 3H); ^{13}C NMR ($CDCl_3$): δ 174.6, 172.6, 169.2, 168.8, 166.9, 157.2, 144.2, 137.6, 131.5, 128.5, 126.9, 122.7, 110.2, 108.1, 74.0, 70.3, 62.3, 55.7, 48.1, 42.3, 33.8, 25.8, 23.0, 16.5, 14.9; LC-HRMS: $t_R = 1.35$ min, [M + H]/z = 511.2556 ($C_{27}H_{35}N_4O_6$), found = 511.2563; UV(MeOH): 255(27200), ε_{290}(4600).

*4.1.2.3. N-((S)-3-{4-[5-(6-Cyclopentyloxy-5-methyl-pyridin-3-yl)-1,2,4-oxadiazol-3-yl]-2-ethyl-6-methyl-phenoxy}-2-hydroxy-propyl)-2-hydroxy-acetamide (**45b**).* Method A, 25%, white solid (42 mg); LC–MS**: $t_R = 1.45$ min, $[M + 1]^+ = 511.3$; ^{1}H NMR ($CDCl_3$): δ 8.86 (d, $J = 2.3$ Hz, 1H), 8.15 (d, $J = 2.3$ Hz, 1H), 7.88 (d, $J = 1.8$ Hz, 1H), 7.86 (d, $J = 1.6$ Hz, 1H), 6.96 (t br, $J = 5.0$ Hz, 1H), 5.57–5.62 (m, 1H), 4.19–4.26 (m, 3H), 3.90 (dd, $J_1 = 4.6$ Hz, $J_2 = 9.5$ Hz, 1H), 3.85 (dd, $J_1 = 6.3$ Hz, $J_2 = 9.6$ Hz, 1H), 3.81 (ddd, $J_1 = 3.1$ Hz, $J_2 = 6.7$ Hz, $J_3 = 14.0$ Hz, 1H), 3.50–3.57 (m, 1H), 3.28 (s br, 1H), 2.75 (q, $J = 7.5$ Hz, 2H), 2.40 (s, 3H), 2.38 (s br, 1H), 2.27 (s, 3H), 1.98–2.08 (m, 2H), 1.80–1.91 (m, 4H), 1.64–1.74 (m, 2H), 1.32 (t, $J = 7.6$ Hz, 3H); ^{13}C NMR ($CDCl_3$): δ 174.3, 172.4, 168.5, 164.6, 157.1, 145.0, 137.6, 137.2, 131.5, 128.4, 126.7, 123.0, 122.2, 113.6, 79.2, 74.0, 70.4, 62.3, 42.2, 33.0, 23.9, 23.0, 16.5, 15.9, 14.9; LC-HRMS: $t_R = 1.53$ min, [M + H]/z = 511.2556 ($C_{27}H_{35}N_4O_6$), found = 511.2561; UV(MeOH): 264(29,100), 285(24,100), ε_{290}(23,700).

*4.1.3. Method B: Preparation of target compounds starting from hydroxy-amidine **8***

*4.1.3.1. N-((S)-3-{2-Ethyl-4-[5-(2-isobutyl-6-methoxy-pyridin-4-yl)-1,2,4-oxadiazol-3-yl]-6-methyl-phenoxy}-2-hydroxy-propyl)-2-hydroxy-acetamide (**7b**)*

(a) A solution of 2-isobutyl-6-methoxyisonicotinic acid **12b** (1.45 g, 5.90 mmol) in DCM (50 mL) DIPEA (3.05 g, 23.6 mmol) followed by TBTU (2.08 g, 6.49 mmol) was added. The mixture was stirred at rt for 5 min before 3-ethyl-*N*,4-dihydroxy-5-methylbenzimidamide **8** [93,96] (1.38 g, 7.08 mmol) dissolved in DMF (5 mL) was added. Stirring was continued at rt for 1 h. The mixture was diluted with DCM (100 mL) and washed with sat. aq. $NaHCO_3$ solution (100 mL) and water (100 mL). The organic extract was dried over $MgSO_4$, filtered and concentrated. The residue was dissolved in dioxane (50 mL) and the solution was stirred at 100 °C for 7 h. The mixture was concentrated and the crude product was purified by CC on silica gel eluting with heptane:EA 4:1 to give 2-ethyl-4-(5-(2-isobutyl-6-methoxypyridin-4-yl)-1,2,4-oxadiazol-3-yl)-6-methylphenol (1.38 g, 64%) as a pale yellow solid; LC–MS: $t_R = 1.18$ min; $[M + 1]^+ = 368.17$; ^{1}H NMR (DMSO-d_6): δ 7.68 (s, 2H), 7.65 (d, $J = 2.3$ Hz, 1H), 7.12 (d, $J = 2.3$ Hz, 1H), 3.94 (s, 3H), 2.66 (q, $J = 7.3$ Hz, 2H), 2.25 (s, 3H), 2.06–2.19 (m, 1H), 1.17 (t, $J = 7.3$ Hz, 3H), 0.91 (d, $J = 6.7$ Hz, 6H).

(b) To a solution of 2-ethyl-4-(5-(2-isobutyl-6-methoxypyridin-4-yl)-1,2,4-oxadiazol-3-yl)-6-methylphenol (100 mg, 272 μmol), PPh_3 (107 mg, 408 μmol), (R)-glycidol (30 mg, 408 μmol) in THF (5 mL), DEAD (178 mg, 408 μmol, as 40% solution in toluene) was added at 5 °C. The mixture was stirred at rt for 3 h before another portion of (R)-glycidol (30 mg, 408 μmol), PPh_3 (107 mg, 408 μmol) and DEAD (178 mg, 408 μmol, as 40% solution in toluene) was added. Stirring was continued at rt for 18 h. The mixture was concentrated and the crude product was purified on prep. TLC plates using heptane:EA 7:3 to give (*S*)-3-(3-ethyl-5-methyl-4-(oxiran-2-ylmethoxy)phenyl)-5-(2-isobutyl-6-methoxypyridin-4-yl)-1,2,4-oxadiazole (88 mg, 76%) as a colourless oil; LC–MS: $t_R = 1.23$ min; $[M + 1]^+ = 424.22$.

(c) A solution of (*S*)-3-(3-ethyl-5-methyl-4-(oxiran-2-ylmethoxy)phenyl)-5-(2-isobutyl-6-methoxypyridin-4-yl)-1,2,4-oxadiazole (72 mg, 170 μmol) in 7 M NH_3 in methanol (5 mL) was stirred in a sealed vessel at 60 °C for 16 h. The mixture was concentrated to give crude (*S*)-1-amino-3-(2-ethyl-4-(5-(2-isobutyl-6-methoxypyridin-4-yl)-1,2,4-oxadiazol-3-yl)-6-methylphenoxy)propan-2-ol (95 mg, quant.) as a colourless oil; LC–MS: $t_R = 0.92$ min; $[M + 1]^+ = 441.26$.

(d) To a solution of the above (*S*)-1-amino-3-(2-ethyl-4-(5-(2-isobutyl-6-methoxypyridin-4-yl)-1,2,4-oxadiazol-3-yl)-6-methylphenoxy)propan-2-ol (95 mg, 170 μmol) in THF, HOBt (32 mg, 237 μmol), glycolic acid (18 mg, 237 μmol), DIPEA (42 mg, 323 μmol) and EDC HCl (46 mg, 237 μmol) was added. The mixture was stirred at rt for 2 h before it was diluted with EA and washed with sat. aq. $NaHCO_3$ solution. The organic extract was concentrated and the crude product was purified on prep. TLC plates using DCM:methanol 10:1 to give the title compound (62 mg, 73%) as a colourless foam; LC–MS: $t_R = 1.42$ min, $[M + 1]^+ = 499.3$; ^{1}H NMR ($CDCl_3$): δ 7.88 (d, $J = 1.8$ Hz, 1H), 7.86 (d, $J = 1.7$ Hz, 1H), 7.46 (d, $J = 1.0$ Hz, 1H), 7.33 (d, $J = 0.9$ Hz, 1H), 7.04 (t, $J = 5.7$ Hz, 1H), 4.19–4.25 (m, 3H), 4.03 (s, 3H), 3.90 (dd, $J_1 = 4.6$ Hz, $J_2 = 9.6$ Hz, 1H), 3.85 (dd, $J_1 = 6.2$ Hz, $J_2 = 9.5$ Hz, 1H), 3.80 (ddd, $J_1 = 3.4$ Hz, $J_2 = 6.7$ Hz, $J_3 = 14.2$ Hz, 1H), 3.50–3.57 (m, 1H), 2.75 (q, $J = 7.5$ Hz, 2H), 2.70 (d, $J = 7.2$ Hz, 2H), 2.39 (s, 3H), 2.23 (hept, $J = 6.7$ Hz, 1H), 1.32 (t, $J = 7.5$ Hz, 3H), 1.00 (d, $J = 6.6$ Hz, 6H); ^{13}C NMR ($CDCl_3$): δ 174.2, 172.7, 168.9, 164.3, 161.5, 157.3, 137.7, 133.7, 131.7, 128.4, 126.7, 122.6, 113.8, 106.0, 74.0, 70.3, 62.3, 54.0, 47.0, 42.3, 28.8, 23.0, 22.5, 16.5, 14.9; LC-HRMS: $t_R = 1.50$ min, [M + H]/z = 499.2556 ($C_{26}H_{35}N_4O_6$), found = 499.2560.

4.2. In vitro potency assessment

GTPγS binding assays were performed in 96 well polypropylene microtiter plates in a final volume of 200 μL. Membrane preparations of CHO cells expressing recombinant human $S1P_1$ or $S1P_3$ receptors were used. Assay conditions were 20 mM Hepes, pH 7.4, 100 mM NaCl, 5 mM $MgCl_2$, 0.1% fatty acid free BSA, 1 or 3 μM GDP (for $S1PR_1$ or $S1PR_3$, respectively), 2.5% DMSO and 50 pM ^{35}S-GTPγS. Test compounds were dissolved and diluted and pre-incubated with the membranes, in the absence of ^{35}S-GTPγS, in 150 μL assay buffer at room temperature for 30 min. After addition of 50 μL of ^{35}S-GTPγS in assay buffer, the reaction mixture was incubated for 1 h at room temperature. The assay was terminated by filtration of the reaction mixture through a Multiscreen GF/C plate, pre-wetted with ice-cold 50 mM Hepes pH 7.4, 100 mM NaCl, 5 mM $MgCl_2$, 0.4% fatty acid free BSA, using a Cell Harvester. The filterplates were then washed with ice-cold 10 mM Na_2HPO_4/NaH_2PO_4 (70%/30%, w/w) containing 0.1% fatty acid free BSA. Then the plates were dried, sealed, 25 μL MicroScint20 was added, and membrane-bound ^{35}S-GTPγS was determined on the TopCount. Specific ^{35}S-GTPγS binding was determined by subtracting non-specific binding (the signal obtained in the absence of agonist)

from maximal binding (the signal obtained with 10 μM S1P). The EC_{50} of a test compound is the concentration of a compound inducing 50% of specific binding. Data (EC_{50}) are given as geometric means.

4.3. Non-GLP 3T3 neutral red uptake phototoxicity assay [76,77]

This test has a good predictability and identifies compounds which act as phototoxic or as photoirritants *in vivo* after systemic or topical application respectively. The 3T3 Neutral Red Uptake (NRU) Phototoxicity assay is a 96-well cytotoxicity-based assay that utilizes normal BALB/c 3T3 mouse fibroblasts to measure the concentration-dependent reduction in neutral red (a vital dye) uptake by the cells one day after treatment with the chemical either in the presence or absence of a non-cytotoxic dose of UVA radiation. Balb/c 3T3 cells, clone 31 (ECACC #86110401; C207 in BioToolBox) were cultured overnight in 96-well microtiter plates with a density of 1×10^4 cells/100 μL in Dulbecco's modified Eagle's medium (DMEM, Invitrogen #21969) containing 10% new born calf serum (NBCS, PAA #B15-102), 4 mM L-glutamine (Invitrogen #25030), 100 U/ml penicillin and 100 μg/mL streptomycin (Invitrogen #15140). The next day, the medium is removed and the cells were washed with phosphate buffered saline containing $CaCl_2$ and $MgCl_2$ (PBS^{++}) (Gibco by life technologies™, #14080). Duplicate 96-well monolayers of 3T3 fibroblasts are exposed to eight different concentrations (0.05–100 μM in DMSO) of chemical with a pre-incubation time of 1 h (at 37 °C, 5% CO_2). One of the plates is exposed to 4 J/cm^2 UVA (1.7 mW/cm^2 for 40 min) almost devoid of UVB (0% transmission at 300 nm, 2.2% at 310 nm, 17.3% at 320 nm, 44.8% at 330 nm, 67.8% at 340 nm, 80% at 350 nm) using the UV-sun simulator UVACUBE 400 equipped with a SOL500 lamp and an H1-Filter (H1 Filter and frame: Cat. Number 4730, Dr. Hönle UV Technology) while the other plate is kept in the dark (-UVA). After UV exposure, PBS^{++} was replaced with culture medium and cell viability is assessed after 24 h with plate-reader at 540 nm. The Neutral Red Uptake (NRU) by cells exposed to the test chemical in the presence of UVA exposure (+UVA) is compared to the NRU by cells exposed to the test chemical in the absence of UVA exposure (−UVA). Dose-response curves were constructed for each experiment and the EC_{50} (+UVA) and EC_{50} (−UVA) values are calculated, i.e. the effective concentration inhibiting cell viability by 50% of untreated controls in the presence and absence of UVA exposure. Chlorpromazine (Sigma–Aldrich #C0982-5G) served as the positive control. A Photo Irritancy Factor (PIF) is then calculated as the ratio of toxicity for each tested chemical with and without UVA according to the formula PIF = EC_{50} (−UVA)/EC_{50} (+UVA). In our case, a PIF >2.5 was considered to be predictive for phototoxic potential. EC_{50} values were calculated geometric means.

4.4. In vivo efficacy

In vivo efficacy of the target compounds was assessed by measuring the circulating lymphocytes after oral administration of 10 mg/kg of a target compound to male Wistar rats (RccHan:WIST) obtained from Harlan Laboratories (Venray, the Netherlands). The animals were housed in climate-controlled conditions with a 12 h-light/dark cycle, and had free access to normal rat chow and drinking water. Blood was collected under isoflurane anaesthesia by sublingual vein puncture before and 3, 6 and 24 h after drug administration. Full blood was subjected to haematology using Beckman Coulter Ac·T 5diff CP (Beckman Coulter International SA, Nyon, Switzerland). All data are presented as mean of 6–8 animals. For formulation, the compounds were dissolved in DMSO. This solution was added to a stirred solution of succinylated gelatine (7.5%) in water. The resulting milky suspension containing a final concentration of 5% of DMSO was administered to the animals by gavage.

4.5. Pharmacokinetics in the rat

Blood samples were obtained from the above *in vivo* efficacy experiments in vials containing EDTA as anticoagulant and plasma was prepared by centrifugation at 3000 g for 10 min at 4 °C. Plasma samples were analyzed using liquid chromatography coupled to mass spectrometry (LC–MS/MS) after protein precipitation. Pharmacokinetic parameters were estimated with the Phoenix WinNonlin 6.3 software package (Pharsight) using non-compartmental analysis.

4.6. Physiology based pharmacokinetic modelling

Chemical structures were loaded into GastroPlus™ v. 7 (Simulations Plus Inc.) and Vss was predicted using the PBPKPlus module, using the default 250 g rat physiology, based on log D and plasma protein binding and blood-to-plasma partitioning, predicted by the ADMET predictor module.

Conflict of interest

The authors declare no competing financial interest.

Acknowledgements

The authors gratefully acknowledge their colleagues and co-workers Lucy Baumann, Maxime Boucher, Céline Bortolamiol, Stéphane Delahaye, Alexandre Flock, Elvire Fournier, Julien Grimont, Hakim Hadana, Julie Hoerner, Benedikt Hofstetter, Matthias Merrettig, Christine Metzger, Sylvie Poirey, Michel Rauser, Manuela Schläpfer, Jürgen Seifert, Virginie Sippel, Gaby von Aesch, Aude Weigel, and Rolf Wüst for the excellent work done and Martine Clozel for support.

Appendix A. Supplementary data

Supplementary data related to this article can be found at http://dx.doi.org/10.1016/j.ejmech.2016.03.020.

References

[1] V.A. Blaho, T. Hla, An update on the biology of sphingosine 1-phosphate receptors, J. Lipid. Res. 55 (2014) 1596–1608.
[2] T. Hla, V. Brinkmann, Sphingosine 1-phosphate (S1P): physiology and the effects of S1P receptor modulation, Neurology 76 (2011) S3–S8.
[3] S.E. Alvarez, S. Milstien, S. Spiegel, Autocrine and paracrine roles of sphingosine-1-phosphate, Trends Endocrinol. Metab. 18 (2007) 300–307.
[4] V. Brinkmann, Sphingosine 1-phosphate receptors in health and disease: mechanistic insights from gene deletion studies and reverse pharmacology, Pharmacol. Ther. 115 (2007) 84–105.
[5] M. Bigaud, D. Guerini, A. Billich, F. Bassilana, V. Brinkmann, Second generation S1P pathway modulators: research strategies and clinical developments, Biochim. Biophys. Acta 1841 (2014) 745–758.
[6] C. Bode, S.-C. Sensken, U. Peest, G. Beutel, F. Thol, B. Levkau, Z. Li, R. Bittman, T. Huang, M. Toelle, M.v.d. Giet, M.H. Graeler, Erythrocytes serve as a reservoir for cellular and extracellular sphingosine 1-phosphate, J. Cell. Biochem. 109 (2010) 1232–1243.
[7] H. Obinata, T. Hla, Sphingosine 1-phosphate in coagulation and inflammation, Semin. Immunopathol. 34 (2012) 73–91.
[8] A.J. Morris, S. Selim, A. Salous, S.S. Smyth, Blood relatives: dynamic regulation of bioactive lysophosphatidic acid and sphingosine-1-phosphate metabolism in the circulation, Trends Cardiovasc. Med. 19 (2009) 135–140.
[9] T. Hla, K. Venkataraman, J. Michaud, The vascular S1P gradient – cellular sources and biological significance, Biochim. Biophys. Acta 1781 (2008) 477–482.
[10] H. LeStunff, P. Giussani, M. Maceyka, S. Lépine, S. Milstien, S. Spiegel, Recycling of sphingosine is regulated by the concerted actions of sphingosine-1-phosphate phosphohydrolase 1 and sphingosine kinase 2, J. Biol. Chem. 282

(2007) 34372–34380.
[11] T. Baumruker, A. Billich, Sphingolipids in cell signalling: their function as receptor ligands, second messengers, and raft constituents, Curr. Immunol. Rev. 2 (2006) 101–118.
[12] T. Okada, T. Kajimoto, S. Jahangeer, S. Nakamura, Sphingosine kinase/sphingosine 1-phosphate signalling in central nervous system, Cell. Signal. 21 (2009) 7–13.
[13] S. Milstien, D. Gude, S. Spiegel, Sphingosine 1-phosphate in neural signalling and function, Acta Paed. 96 (2007) 40–43.
[14] V. Brinkmann, T. Baumruker, Pulmonary and vascular pharmacology of sphingosine 1-phosphate, Curr. Opin. Pharmacol. 6 (2006) 244–250.
[15] S. Uhlig, E. Gulbins, Sphingolipids in the lungs, Am. J. Respir. Crit. Care Med. 178 (2008) 1100–1114.
[16] A.E. Alewijnse, S.L.M. Peters, Sphingolipid signalling in the cardiovascular system: good, bad or both? Eur. J. Pharmacol. 585 (2008) 292–302.
[17] H. Rosen, M.G. Sanna, S.M. Cahalan, P.J. Gonzalez-Cabrera, Tipping the gatekeeper: S1P regulation of endothelial barrier function, Trends Immunol. 28 (2007) 102–107.
[18] B.J. McVerry, J.G.N. Garcia, In vitro and in vivo modulation of vascular barrier integrity by sphingosine 1-phosphate: mechanistic insights, Cell. Signal. 17 (2005) 131–139.
[19] M. Ishii, J.G. Egen, F. Klauschen, M. Meier-Schellersheim, Y. Saeki, J. Vacher, R.L. Proia, R.N. Germain, Sphingosine-1-phosphate mobilizes osteoclast precursors and regulates bone homeostasis, Nature 458 (2009) 524–528.
[20] M.L. Allende, G. Tuymetova, B.G. Lee, E. Bonifacino, Y.-P. Wu, R.L. Proia, $S1P_1$ receptor directs the release of immature B cells from bone marrow into blood, J. Exp. Med. 207 (2010) 1113–1124.
[21] M.M. Price, D. Kapitonov, J. Allegood, S. Milstien, C.A. Oskeritzian, S. Spiegel, Sphingosine-1-phosphate induces development of functionally mature chymase-expressing human mast cells from hematopoietic progenitors, FASEB J. 23 (2009) 3506–3515.
[22] J. Rivera, R.L. Proia, A. Olivera, The alliance of sphingosine-1-phosphate and its receptors in immunity, Nat. Rev. Immunol. 8 (2008) 753–763.
[23] C.A. Oskeritzian, S. Milstien, S. Spiegel, Sphingosine-1-phosphate in allergic responses, asthma and anaphylaxis, Pharmacol. Ther. 115 (2007) 390–399.
[24] V. Brinkmann, M.D. Davis, C.E. Heise, R. Albert, S. Cottens, R. Hof, C. Bruns, E. Prieschl, T. Baumruker, P. Hiestand, C.A. Foster, M. Zollinger, K.R. Lynch, The immune modulator FTY720 targets sphingosine 1-Phosphate receptors, J. Biol. Chem. 277 (2002) 21453–21457.
[25] S. Mandala, R. Hajdu, J. Bergstrom, E. Quackenbush, J. Xie, J. Milligan, R. Thornton, G.-J. Shei, D. Card, C.A. Keohane, M. Rosenbach, J. Hale, C.L. Lynch, K. Rupprecht, W. Parsons, H. Rosen, Alteration of lymphocyte trafficking by sphingosine-1-phosphate receptor agonists, Science 296 (2002) 346–349.
[26] D.D. Pinschewer, A.F. Ochsenbein, B. Odermatt, V. Brinkmann, H. Hengartner, R.M. Zinkernagel, FTY720 immunosupression impairs effector T cell peripheral homing without affecting induction, expansion, and memory, J. Immunol. 164 (2000) 5761–5770.
[27] V. Brinkmann, S. Chen, L. Feng, D. Pinschewer, Z. Nikolova, R. Hof, FTY720 alters lymphocyte homing and protects allografts without inducing general immunosuppression, Transplant. Proc. 33 (2001) 530–531.
[28] J.G. Cyster, S.R. Schwab, Sphingosine-1-phosphate and lymphocyte egress from lymphoid organs, Ann. Rev. Immunol. 30 (2012) 69–94.
[29] V. Brinkmann, K.R. Lynch, FTY720: targeting G-protein-coupled receptors for sphingosine 1-phosphate in transplantation and autoimmunity, Curr. Opin. Immunol. 14 (2002) 569–575.
[30] D.M. Wingerchuk, J.L. Carter, Multiple sclerosis: current and emerging disease-modifying therapies and treatment strategies, Mayo Clin. Proc. 89 (2014) 225–240.
[31] A. Groves, Y. Kihara, J. Chun, Fingolimod: direct CNS effects of sphingosine 1-phosphate (S1P) receptor modulation and implications in multiple sclerosis therapy, J. Neurol. Sci. 328 (2013) 9–18.
[32] J. Ingwersen, O. Aktas, P. Kuery, B. Kieseier, A. Boyko, H.-P. Hartung, Fingolimod in multiple sclerosis: mechanisms of action and clinical efficacy, Clin. Immunol. 142 (2012) 15–24.
[33] J.A. Cohen, J. Chun, Mechanisms of fingolimod's efficacy and adverse effects in multiple sclerosis, Ann. Neurol. 69 (2011) 759–777.
[34] L. Kappos, E.-W. Radue, P. O'Connor, C. Polman, R. Hohlfeld, P. Calabresi, K. Selmaj, C. Agoropoulou, M. Leyk, L. Zhang-Auberson, P. Burtin, A placebo-controlled trial of oral fingolimod in relapsing multiple sclerosis, N. Engl. J. Med. 362 (2010) 387–401.
[35] A. Vaclavkova, S. Chimenti, P. Arenberger, P. Hollo, P.G. Sator, M. Burcklen, M. Stefani, D. D'Ambrosio, Oral ponesimod in patients with chronic plaque psoriasis: a randomised, double-blind, placebo-controlled phase 2 trial, Lancet 384 (2014) 2036–2045.
[36] ClinicalTrials.gov, Efficacy and Tolerability of BAF312 in Patients with Polymyositis and Dermatomyositis, 2012.
[37] ClinicalTrials.gov, Efficacy and Safety Study of RPC1063 in Ulcerative Colitis, 2012.
[38] ClinicalTrials.gov, Safety and Efficacy of KRP203 in Subacute Cutaneous Lupus Erythematosus, 2012.
[39] ClinicalTrials.gov, Efficacy & Safety in Moderately Active Refractory Ulcerative Colitis Patients, 2012.
[40] ClinicalTrials.gov, Efficacy, Tolerability, Pharmacokinetcs and Pharmacodynamics Study of MT-1303 in Subjects with Inflammatory Bowel Disease, 2012.
[41] J. Gatfield, L. Monnier, R. Studer, M.H. Bolli, B. Steiner, O. Nayler, Sphingosine-1-phosphate (S1P) displays sustained S1P receptor agonism and signaling through S1P lyase-dependent receptor recycling, Cell Signal. 26 (2014) 1576–1588.
[42] F. Mullershausen, F. Zecri, C. Cetin, A. Billich, D. Guerini, K. Seuwen, Persistent signaling induced by FTY720-phosphate is mediated by internalized S1P1 receptors, Nat. Chem. Biol. 5 (2009) 428–434.
[43] K. Chiba, FTY720, a new class of immunomodulator, inhibits lymphocyte egress from secondary lymphoid tissues and thymus by agonistic activity at sphingosine 1-phosphate receptors, Pharmacol. Ther. 108 (2005) 308–319.
[44] E. Jo, M.G. Sanna, P.J. Gonzalez-Cabrera, S. Thangada, G. Tigyi, D.A. Osborne, T. Hla, A.L. Parrill, H. Rosen, S1P1-selective in vivo-active agonists from high-throughput screening: off-the-shelf chemical probes of receptor interactions, signaling, and fate, Chem. Biol. 12 (2005) 703–715.
[45] M.H. Gräler, E.J. Goetzl, The immunosuppressant FTY720 down-regulates sphingosine 1-phosphate G-protein-coupled receptors, FASEB J. 18 (2004) 551–553.
[46] S.M. Cahalan, P.J. Gonzalez-Cabrera, N. Nguyen, M. Guerrero, E.A. Cisar, N.B. Leaf, S.J. Brown, E. Roberts, H. Rosen, Sphingosine 1-phosphate receptor 1 (S1P(1)) upregulation and amelioration of experimental autoimmune encephalomyelitis by an S1P(1) antagonist, Mol. Pharmacol. 83 (2013) 316–321.
[47] J. Quancard, B. Bollbuck, P. Janser, D. Angst, F. Berst, P. Buehlmayer, M. Streiff, C. Beerli, V. Brinkmann, D. Guerini, P.A. Smith, T.J. Seabrook, M. Traebert, K. Seuwen, R. Hersperger, C. Bruns, F. Bassilana, M. Bigaud, A potent and selective $S1P_1$ antagonist with efficacy in experimental autoimmune encephalomyelitis, Chem. Biol. 19 (2012) 1142–1151.
[48] D. Angst, P. Janser, J. Quancard, P. Buehlmayer, F. Berst, L. Oberer, C. Beerli, M. Streiff, C. Pally, R. Hersperger, C. Bruns, F. Bassilana, B. Bollbuck, An oral sphingosine 1-phosphate receptor 1 ($S1P_1$) antagonist prodrug with efficacy in vivo: discovery, synthesis, and evaluation, J. Med. Chem. 55 (2012) 9722–9734.
[49] Y. Fujii, H. Ohtake, N. Ono, T. Hara, T. Sakurai, S. Takahashi, T. Takayama, Y. Fukasawa, F. Shiozawa, N. Tsukahara, T. Hirayama, Y. Igarashi, R. Goitsuka, Lymphopenia induced by a novel selective $S1P_1$ antagonist structurally unrelated to S1P, Biochim. Biophys. Acta 1821 (2012) 600–606.
[50] G. Tarrasón, M. Aulí, S. Mustafa, V. Dolgachev, M.T. Domènech, N. Prats, M. Domínguez, R. López, N. Auilar, M. Calbet, M. Pont, G. Milligan, S.L. Kunkel, N. Godessart, The sphingosine-1-phosphate receptor-1 antagonist, W146, causes early and short-lasting peripheral blood lymphophenia in mice, Int. Immunopharmacol. 11 (2011) 1773–1779.
[51] S. Weiler, N. Braendlin, C. Beerli, C. Bergsdorf, A. Schubart, H. Srinivas, B. Oberhauser, A. Billich, Orally active 7-substituted (4-benzyl-phthalazin-1-yl)-2-methyl-piperazin-1-yl]-nicotinonitriles as active-site inhibitors of sphingosine-1-phosphate lyase for the treatment of multiple sclerosis, J. Med. Chem. 57 (2014) 5074–5084.
[52] M. Mori, S. Kuwabara, Are more sphingosine 1-phosphate receptor agonists a better therapeutic option against multiple sclerosis? J. Neurol. Neurosurg. Psychiatry 85 (2014) 1180.
[53] H. Obinata, T. Hla, Fine-tuning S1P therapeutics, Chem. Biol. 19 (2012) 1080–1082.
[54] M.L. Allende, J.L. Dreier, S. Mandala, R.L. Proia, Expression of the sphingosine 1-phosphate receptor, $S1P_1$, on T-cells controls thymic emigration, J. Biol. Chem. 279 (2004) 15396–15401.
[55] M. Matloubian, C.G. Lo, G. Cinamon, M.J. Lesneski, Y. Xu, V. Brinkmann, M.L. Allende, R.L. Proia, J.G. Cyster, Lymphocyte egress from thymus and peripheral lymphoid organs is dependent on S1P receptor 1, Nature 427 (2004) 355–360.
[56] S.H. Wei, H. Rosen, M.P. Matheu, M.G. Sanna, S.-K. Wang, E. Jo, C.-H. Wong, I. Parker, M.D. Cahalan, Sphingosine 1-phosphate type 1 receptor agonism inhibits transendothelial migration of medullary T cells to lymphatic sinuses, Nat. Immunol. 6 (2005) 1228–1235.
[57] J.J. Hale, W. Neway, S.G. Mills, R. Hajdu, C.A. Keohane, M. Rosenbach, J. Milligan, G.-J. Shei, G. Chrebet, J. Bergstrom, D. Card, G.C. Koo, S.L. Koprak, J.J. Jackson, H. Rosen, S. Mandala, Potent S1P receptor agonists replicate the pharmacologic actions of the novel immune modulator FTY720, Bioorg. Med. Chem. Lett. 14 (2004) 3351–3355.
[58] M.G. Sanna, J. Liao, E. Jo, C. Alfonso, M.-Y. Ahn, M.S. Peterson, B. Webb, S. Lefebvre, J. Chun, N. Gray, H. Rosen, Sphingosine 1-Phosphate (S1P) receptor subtypes $S1P_1$ and $S1P_3$, respectively, regulate lymphocyte recirculation and heart rate, J. Biol. Chem. 279 (2004) 13839–13848.
[59] N. Seki, Y. Maeda, H. Kataoka, K. Sugahara, T. Sugita, K. Chiba, Fingolimod (FTY720) ameliorates experimental autoimmune encephalomyelitis (EAE): II. FTY720 decreases infiltration of Th17 and Th1 cells into the central nervous system in EAE, Inflamm. Regen. 30 (2010) 542–548.
[60] H. Kataoka, K. Sugahara, K. Shimano, K. Teshima, M. Koyama, A. Fukunari, K. Chiba, FTY720, sphingosine 1-phosphate receptor modulator, ameliorates experimental autoimmune encephalomyelitis by inhibition of T cell infiltration, Cell. Mol. Immunol. 2 (2005) 439–448.
[61] M. Webb, C.S. Tham, F.F. Lin, K. Lariosa-Willingham, N. Yu, J. Hale, S. Mandala, J. Chun, T.S. Rao, Sphingosine 1-phosphate receptor agonists attenuate relapsing-remitting experimental autoimmune encephalitis in SJL mice, J. Neuroimmunol. 153 (2004) 108–121.
[62] P.J. Gonzalez-Cabrera, S.M. Cahalan, N. Nguyen, G. Sarkisyan, N.B. Leaf, M.D. Cameron, T. Kago, H. Rosen, S1P1 receptor modulation with cyclical recovery from lymphopenia amelioreates mouse model of multiple sclerosis,

Mol. Pharmacol. 81 (2012) 166–174.
[63] J.W. Choi, S.E. Gardell, D.R. Herr, R. Rivera, C.-W. Lee, K. Noguchi, S.T. Teo, Y.C. Yung, M. Lu, G. Kennedy, J. Chun, FTY720 (fingolimod) efficacy in an animal model of multiple sclerosis requires astrocyte sphingosine 1-phosphate receptor 1 ($S1P_1$) modulation, Proc. Natl. Acad. Sci. U. S. A. 108 (2011) 751–756.
[64] B. Balatoni, M.K. Storch, E.M. Swoboda, V. Schonborn, A. Koziel, G.N. Lambrou, P.C. Hiestand, R. Weissert, C.A. Foster, FTY720 sustains and restores neuronal function in the DA rat model of MOG-induced experimental autoimmune encephalomyelitis, Brain Res. Bull. 74 (2007) 307–316.
[65] V.E. Miron, S.K. Ludwin, P.J. Darlington, A.A. Jarjour, B. Soliven, T.E. Kennedy, J.P. Antel, Fingolimod (FTY720) enhances remyelination following demyelination of organotypic cerebellar slices, Am. J. Pathol. 176 (2010) 2682–2694.
[66] A. Murakami, H. Taksugi, S. Ohnuma, Y. Koide, A. Sakurai, S. Takeda, T. Hasegawa, J. Sasamori, T. Konno, K. Hayashi, Y. Watanabe, K. Mori, Y. Sato, A. Takahashi, N. Mochizuki, N. Takakura, Sphingosine 1-phosphate (S1P) regulates vascular contraction via $S1P_3$ receptor: investigation based on a new $S1P_3$ receptor antagonist, Mol. Pharmacol. 77 (2010) 704–713.
[67] J.J. Hale, G. Doherty, L. Toth, S.G. Mills, R. Hajdu, C.A. Keohane, M. Rosenbach, J. Milligan, G.-J. Shei, G. Chrebet, J. Bergstrom, D. Card, M. Forrest, S.-Y. Sun, S. West, H. Xie, N. Nomura, H. Rosen, S. Mandala, Selecting against $S1P_3$ enhances the acute cardiovascular tolerability of 3-(N-benzyl)aminopropylphosphonic acid S1P receptor agonists, Bioorg. Med. Chem. Lett. 14 (2004) 3501–3505.
[68] M. Forrest, S.-Y. Sun, R. Hajdu, J. Bergstrom, D. Card, G. Doherty, J. Hale, C. Keohane, C. Meyers, J. Milligan, S. Mills, N. Nomura, H. Rosen, M. Rosenbach, G.-J. Shei, I.I. Singer, M. Tian, S. West, V. White, J. Xie, R.L. Proia, S. Mandala, Immune cell regulation and cardiovascular effects of sphingosine 1-phosphate receptor agonists in rodents are mediated via distinct receptor subtypes, J. Pharmacol. Exp. Ther. 309 (2004) 758–768.
[69] S. Salomone, E.M. Potts, S. Tyndall, P.C. Ip, J. Chun, V. Brinkmann, C. Waeber, Analysis of sphingosine 1-phosphate receptors involved in constriction of isolated cerebral arteries with receptor null mice and pharmacological tools, Brit. J. Pharmacol. 153 (2008) 140–147.
[70] R.M. Fryer, A. Muthukumarana, P.C. Harrison, S. Nodop Mazurek, R.R. Chen, K.E. Harrington, R.M. Dinallo, J.C. Horan, L. Patnaude, L.K. Modis, G.A. Reinhart, The clinically-tested S1P receptor agonists, FTY720 and BAF312, demonstrate subtype-specific bradycardia (S1P(1)) and hypertension (S1P(3)) in rat, PLoS One 7 (2012) e52985.
[71] K. Sobel, K. Menyhart, N. Killer, B. Renault, Y. Bauer, R. Studer, B. Steiner, M.H. Bolli, O. Nayler, J. Gatfield, Sphingosine-1-phosphate (S1P) receptor agonists mediate pro-fibrotic responses in normal human lung fibroblasts via $S1P_2$ and $S1P_3$ receptors and Smad-independent signaling, J. Biol. Chem. 288 (2013) 14839–14851.
[72] M. Urbano, M. Guerrero, H. Rosen, E. Roberts, Modulators of the sphingosine 1-phosphate receptor 1, Bioorg. Med. Chem. Lett. 23 (2013) 6377–6389.
[73] E. Roberts, M. Guerrero, M. Urbano, H. Rosen, Sphingosine 1-phosphate receptor agonists: a patent review (2010–2012), Exp. Opin. Ther. Pat. 23 (2013) 817–841.
[74] M.H. Bolli, C. Lescop, O. Nayler, Synthetic sphingosine 1-phosphate receptor modulators – opportunities and potential pitfalls, Curr. Top. Med. Chem. 11 (2011) 726–757.
[75] M.H. Bolli, S. Abele, M. Birker, R. Bravo, D. Bur, R. de Kanter, C. Kohl, J. Grimont, P. Hess, C. Lescop, B. Mathys, C. Muller, O. Nayler, M. Rey, M. Scherz, G. Schmidt, J. Seifert, B. Steiner, J. Velker, T. Weller, Novel S1P1 receptor agonists – part 3: from thiophenes to pyridines, J. Med. Chem. 57 (2014) 110–130.
[76] H. Spielmann, M. Balls, J. Dupuis, W.J. Pape, G. Pechovitch, O. de Silva, H.G. Holzhutter, R. Clothier, P. Desolle, F. Gerberick, M. Liebsch, W.W. Lovell, T. Maurer, U. Pfannenbecker, J.M. Potthast, M. Csato, D. Sladowski, W. Steiling, P. Brantom, The international EU/COLIPA in vitro phototoxicity validation study: results of phase II (blind trial). Part 1: the 3T3 NRU phototoxicity test, Toxicol. In Vitro 12 (1998) 305–327.
[77] B. Peters, H.G. Holzhutter, In vitro phototoxicity testing: development and validation of a new concentration response analysis software and biostatistical analyses related to the use of various prediction models, Altern. Lab. Anim. 30 (2002) 415–432.
[78] A.M. Lynch, P. Wilcox, Review of the performance of the 3T3 NRU in vitro phototoxicity assay in the pharmaceutical industry, Exp. Toxicol. Pathol. 63 (2011) 209–214.
[79] M. Bolli, D. Lehmann, B. Mathys, C. Mueller, O. Nayler, B. Steiner, J. Velker, in: Pyridine-3-yl Derivatives as Immunomodulating Agents, Actelion Pharmaceuticals Ltd., 2008.
[80] Food and Drug Administration, in: S10 Photosafety Evaluation of Pharmaceuticals, Center for Drug Evaluation and Research (CDER), 2012.
[81] European Medicine Agency, in: ICH Guideline S10 Guidance on Photosafety Evaluation of Pharmaceuticals, Committee for Medicinal Products for Human Use, 2012.
[82] Y. Haranosono, M. Kurata, H. Sakaki, Establishment of an in silico phototoxicity prediction method by combining descriptors related to photo-absorption and photo-reaction, J. Toxicol. Sci. 39 (2014) 655–664.
[83] A. Fürstner, A. Leitner, Iron-catalyzed cross-coupling reactions of alkyl-Grignard reagents with aryl chloride, tosylates and triflates, Angew. Chem. Int. Ed. 41 (2002) 609–612.
[84] A. Fürstner, A. Leitner, M. Méndez, H. Krause, Iron-catalyzed cross coupling reactions, J. Am. Chem. Soc. 124 (2002) 13856–13863.
[85] H. Matsushita, E. Negishi, Palladium-catalyzed reactions of allylic electrophiles with organometallic reagents. A regioselective 1,4-elimination and a regio- and stereoselective reduction of allylic derivatives, J. Org. Chem. 47 (1982) 4161–4165.
[86] J.A. Casares, P. Espinet, B. Fuentes, G. Salas, Insights into the mechanism of the Negishi reaction: ZnRX versus ZnR2 reagents, J. Am. Chem. Soc. 129 (2007) 3508–3509.
[87] C.C.C. Johansson Seechurn, M.O. Kitching, T.J. Colacot, V. Snieckus, Palladium-catalyzed cross-coupling: a historical contextual perspective to the 2010 nobel prize, Angew. Chem. Int. Ed. Engl. 51 (2012) 5062–5085.
[88] H. Doucet, Suzuki–Miyaura cross-coupling reactions of alkylboronic acid derivatives or alkyltrifluoroborates with aryl, alkenyl or alkyl halides and triflates, Eur. J. Org. Chem. 2008 (2008) 2013–2030.
[89] J.T. Binder, C.J. Cordier, G.C. Fu, Catalytic enantioselective cross-couplings of secondary alkyl electrophiles with secondary alkylmetal nucleophiles: Negishi reactions of racemic benzylic bromides with achiral alkylzinc reagents, J. Am. Chem. Soc. 134 (2012) 17003–17006.
[90] Z. Liu, N. Dong, M. Xu, Z. Sun, T. Tu, Mild Negishi cross-coupling reactions catalyzed by acenaphthoimidazolylidene palladium complexes at low catalyst loadings, J. Org. Chem. 78 (2013) 7436–7444.
[91] C. Han, S.L. Buchwald, Negishi coupling of secondary alkylzinc halides with aryl bromides and chlorides, J. Am. Chem. Soc. 131 (2009) 7532–7533.
[92] F. Kerins, D.F. O'Shea, Generation of substituted styrenes via Suzuki cross-coupling of aryl halides with 2,4,6-trivinylcyclotriboroxane, J. Org. Chem. 67 (2002) 4968–4971.
[93] M.H. Bolli, C. Müller, B. Mathys, S. Abele, M. Birker, R. Bravo, D. Bur, P. Hess, C. Kohl, D. Lehmann, O. Nayler, M. Rey, S. Meyer, M. Scherz, G. Schmidt, B. Steiner, A. Treiber, J. Velker, T. Weller, Novel $S1P_1$ receptor agonists – part 1: from pyrazoles to thiophenes, J. Med. Chem. 56 (2013) 9737–9755.
[94] M.H. Bolli, J. Velker, C. Müller, B. Mathys, M. Birker, R. Bravo, D. Bur, R. de Kanter, P. Hess, C. Kohl, D. Lehmann, S. Meyer, O. Nayler, M. Rey, M. Scherz, B. Steiner, Novel $S1P_1$ receptor agonists – part 2: from bicyclo[3.1.0]hexane fused thiophenes to isobutyl substituted thiophenes, J. Med. Chem. 57 (2014) 78–97.
[95] M.H. Bolli, S. Abele, C. Binkert, R. Bravo, S. Buchmann, D. Bur, J. Gatfield, P. Hess, C. Kohl, C. Mangold, B. Mathys, K. Menyhart, C. Müller, O. Nayler, M. Scherz, G. Schmidt, V. Sippel, B. Steiner, D. Strasser, A. Treiber, T. Weller, 2-Imino-thiazolidin-4-one derivatives as potent, orally active S1P1 receptor agonists, J. Med. Chem. 53 (2010) 4198–4211.
[96] G. Schmidt, S. Reber, M.H. Bolli, S. Abele, Practical and scalable synthesis of S1P1 receptor agonist ACT-209905, Org. Proc. Res. Dev. 16 (2012) 595–604.